Nat Hazards
DOI 10.1007/s11069-016-2274-4

ORIGINAL PAPER

Dynamic soil characterization and site response estimation for Erbaa, Tokat (Turkey)

Muge K. Akin[1] · **Steven L. Kramer**[2] · **Tamer Topal**[3]

Received: 4 February 2015 / Accepted: 23 February 2016

Abstract Site amplification is one of the most important factors controlling damage in urban areas through strong earthquakes. Local site effects play an important role in earthquake-resistant design and should be considered for site response analyses. In this study, ground response analyses in Erbaa, Turkey, a settlement in the North Anatolian Fault Zone, using one-dimensional equivalent linear analysis and empirical approaches based on shear wave velocity profiles are evaluated and compared. The ground response analyses were performed with consideration of shear wave velocity, and modulus reduction and damping behavior for different confining pressure and plasticity index-dependent models. The results of ground response analyses and amplification values from empirical equations using shear wave velocity are illustrated in terms of amplification and predominant period maps of the seismically active Erbaa settlement area. The comparison has been made in these produced maps of the study area in order to evaluate different site response analyses.

Keywords Ground response analysis · Soil amplification · Erbaa · Turkey · Site effect · Map

1 Introduction

Soil conditions at a site may increase or amplify bedrock motions by some factor during earthquake shaking. Site effects control the variation of ground surface motion components (amplitude, frequency content and duration) caused by the incoming wave field due to the

✉ Muge K. Akin
mugeakink@gmail.com; muge.akin@agu.edu.tr

[1] Department of Civil Engineering, Abdullah Gul University, Kayseri, Turkey

[2] Department of Civil and Environmental Engineering, University of Washington, Seattle, WA, USA

[3] Department of Geological Engineering, Middle East Technical University, Ankara, Turkey

Published online: 11 March 2016

properties of soil deposits and surface topography (Pitilakis 2004). The amplification case from a site located 97 km from the epicenter of 1989 Loma Prieta earthquake ($M_w = 7.1$) is one of the important amplification cases in the history (Seed et al. 1990). Soft soil conditions in the site amplified bedrock motions by a factor of 2–3 in both time history and spectral acceleration for different periods in this earthquake (Kramer 1996).

Site effects in the form of amplification or de-amplification were observed in many disastrous seismic events in seismogenic areas such as 1985 Michoacan-Mexico (Seed and Sun 1989), 1989 Loma Prieta (Seed et al. 1990), 1994 Northridge (Moehle 1994), 1995 Kobe (Takemiya and Adam 1997), 1999 Kocaeli (Erdik et al. 1985; Tezcan et al. 2002; Ergin et al. 2004; Ozel and Sasatani 2004; Cabalar and Cevik 2009) and 1999 Chi–Chi earthquakes (Pavlenko 2008). The 1985 Michoacan earthquake ($M_s = 8.1$) caused particularly severe damage in Mexico City inside the Mexico Valley, which is approximately 400 km away from the epicenter in the Pacific Ocean. It was one of the great examples to understand the effects of amplification phenomena or the amount of site effects since the seismic waves were very strongly amplified inside the lake-bed zone of the valley (Vucetic and Dobry 1991; Castro et al. 1990; Humphrey and Anderson 1992). Site conditions can be determined by site classifications for ground motion amplification purposes. Site classifications can be determined by means of surface geology, geotechnical data, and/or shear wave velocity, V_{s30}, values to define amplification factors (Kramer and Stewart 2004).

In this study, soil amplification and predominant periods were evaluated by ground response analyses using one-dimensional equivalent linear analyses and empirical approaches based on shear wave velocity profiles. The results of ground response analyses and amplification values from empirical equations using shear wave velocity were considered to produce amplification and predominant period maps of seismically active Erbaa settlement area. A comparison has been made in these produced maps of the study area to evaluate different site response analyses. In order to assess the dynamic soil properties, a geophysical investigation with 24 resistivity, 20 seismic refraction, 30 seismic cone penetration applications, and 10 SPT-based uphole survey methods, and data from geotechnical boreholes was undertaken in the study area.

2 General settings

2.1 Description of the study area

The seismicity of the northern part of Turkey is mainly controlled by the active North Anatolian Fault Zone (NAFZ). The study area, Erbaa, is one of the largest towns of Tokat province and partly located on the Kelkit river plain within NAFZ (Fig. 1). The city center of old Erbaa was on the south side of the Kelkit River. After the disastrous 1942 earthquake ($M_w = 7.2$), the settlement area was seriously damaged and moved farther southwards of its old location in 1944.

2.2 Geology and seismo-tectonics

The study area, Erbaa, and its close vicinity are within a pull-apart basin which was formed by tectonic activity of the North Anatolian Fault Zone (NAFZ). The NAFZ is a 1500-km-long seismically active right lateral strike-slip fault that has a relative motion between the Anatolian Plate and Black Sea Plate (Sengör et al. 1985, 2005; Westaway 2003). Between 1939 and 1967, the NAFZ ruptured by six large, westward-propagating earthquakes with

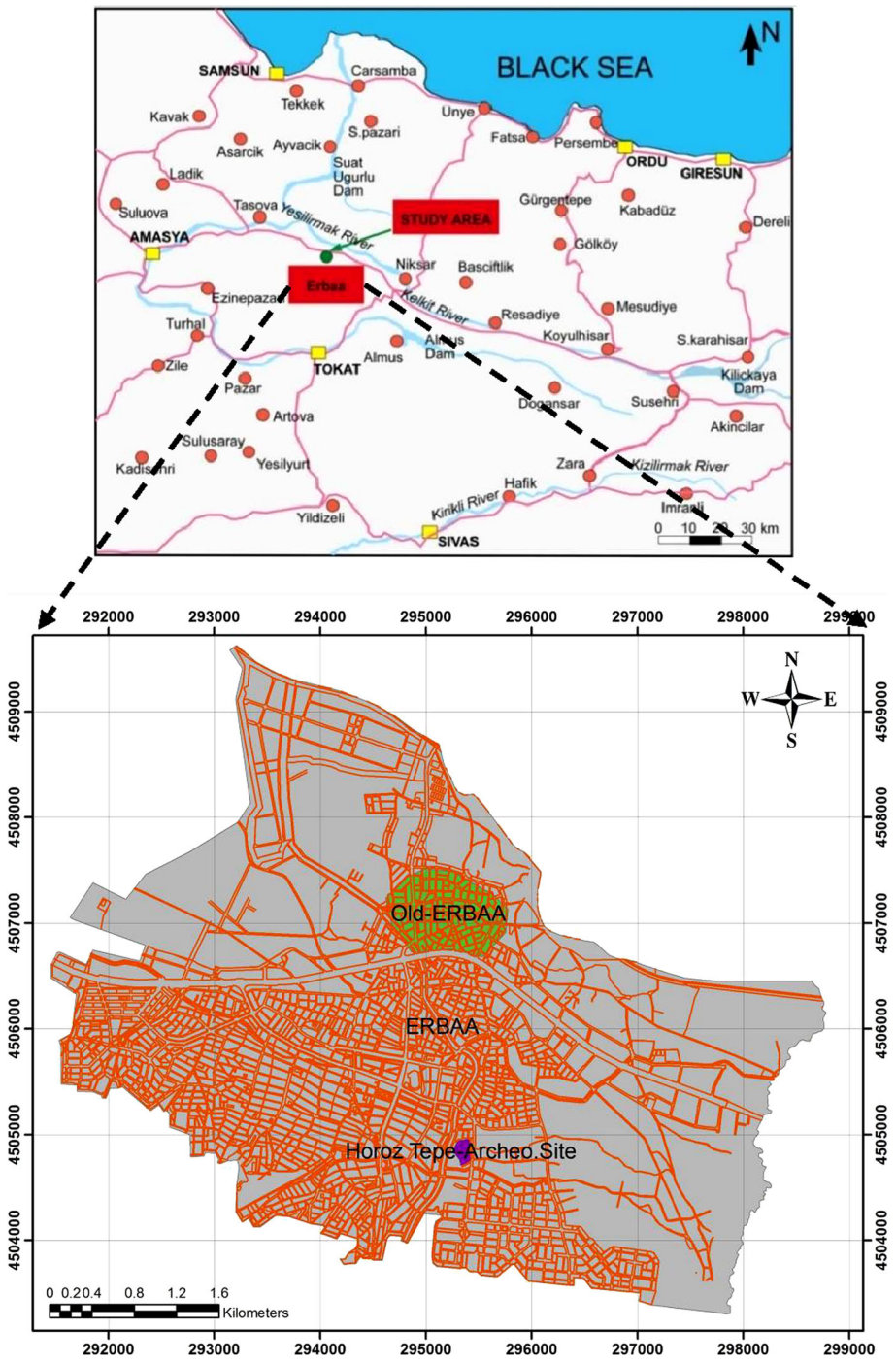

Fig. 1 The location map of the study area

magnitudes >7 and caused approximately 900 km surface break (Allen 1969; Ketin 1969; Ambraseys 1970). The study area, Erbaa, is located on the eastern part of the NAFZ. Surface ruptures of the 1939, 1942 ($M_w = 7.1$ or 7.2) and 1943 ($M_w = 7.6$) earthquakes occurred in the Tasova-Erbaa and Niksar basins (Barka et al. 2000). The Tasova-Erbaa pull-apart basin is approximately 65 km long and 15–18 km wide. According to Barka et al. (2000), there is 700 m of sedimentary fill in this basin that can be seen in the seismo-tectonic map of the area (Fig. 2). The November 26, 1943 Tosya earthquake ($M_w = 7.6$) produced 280-km-long surface rupture, which could be the second longest surface faulting in that sequence (Stein et al. 1997). The southern part of Erbaa is bounded by the Esencay fault, which has a different morphological expression; however, no instrumental and/or historical earthquakes were mentioned in the study of Barka et al. (2000) related to this fault.

Metamorphic rocks and the limestone layers as basement rocks can be observed with an age from Permian to Eocene in the study area in a regional macro scale. These rocks are overlaid by Upper Eocene volcanics (basalt, andesite, agglomerate, and tuff) and the alternation of sandstone siltstone layers. These units are covered by Pliocene deposits consisting of semi-consolidated clay, silt, sand, and gravel with an unconformity and recent Quaternary alluvial unit (Aktimur et al. 1992) (Figs. 2, 3).

The alluvium including gravel, sand, and silty clay can be observed in the basement of Kelkit River valleys and in the northern part of the Erbaa basin. The alluvial unit consists of heterogeneous materials derived from various older geological units in the vicinity. The Quaternary alluvial unit and Pliocene deposits broadly cover the study area. While the northern part of the settlement area is located on the alluvial unit, the Pliocene deposits dominate the southern part of Erbaa (Yılmaz 1998).

The study area is mainly located on the Erbaa basin, which consists of Pliocene and Quaternary deposits (Fig. 3). Erbaa basin is located on the eastern part of the NAFZ and is surrounded by fault segments that ruptured in the 1942 and 1943 earthquakes. The district was firstly located on the Quaternary alluvium and the alluvial fan nearby the Kelkit River before these disastrous earthquakes. After the 1942 earthquake, the settlement had to be moved toward the Pliocene deposits on the southern hills.

During 1900s, several earthquakes occurred in this region. Erbaa is considered in the First Degree Earthquake Zone of Turkey (http://www.deprem.gov.tr/indexen.html). The 1942 Niksar-Erbaa earthquake is the most destructive earthquake for the region. No

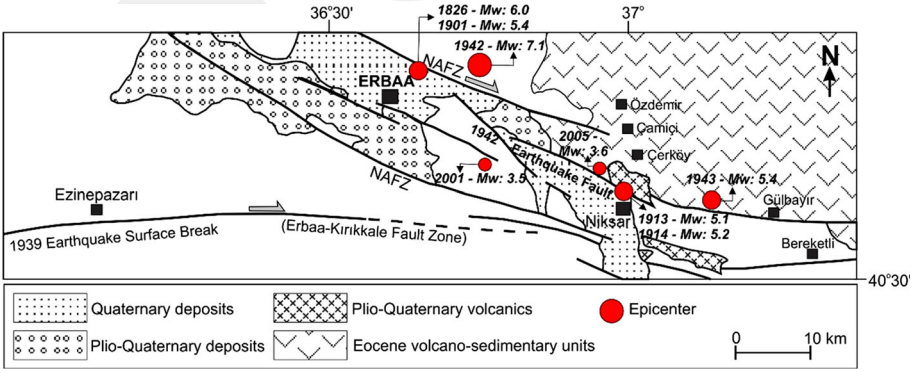

Fig. 2 Seismo-tectonic map of the study area (revised after Tatar et al. 1995)

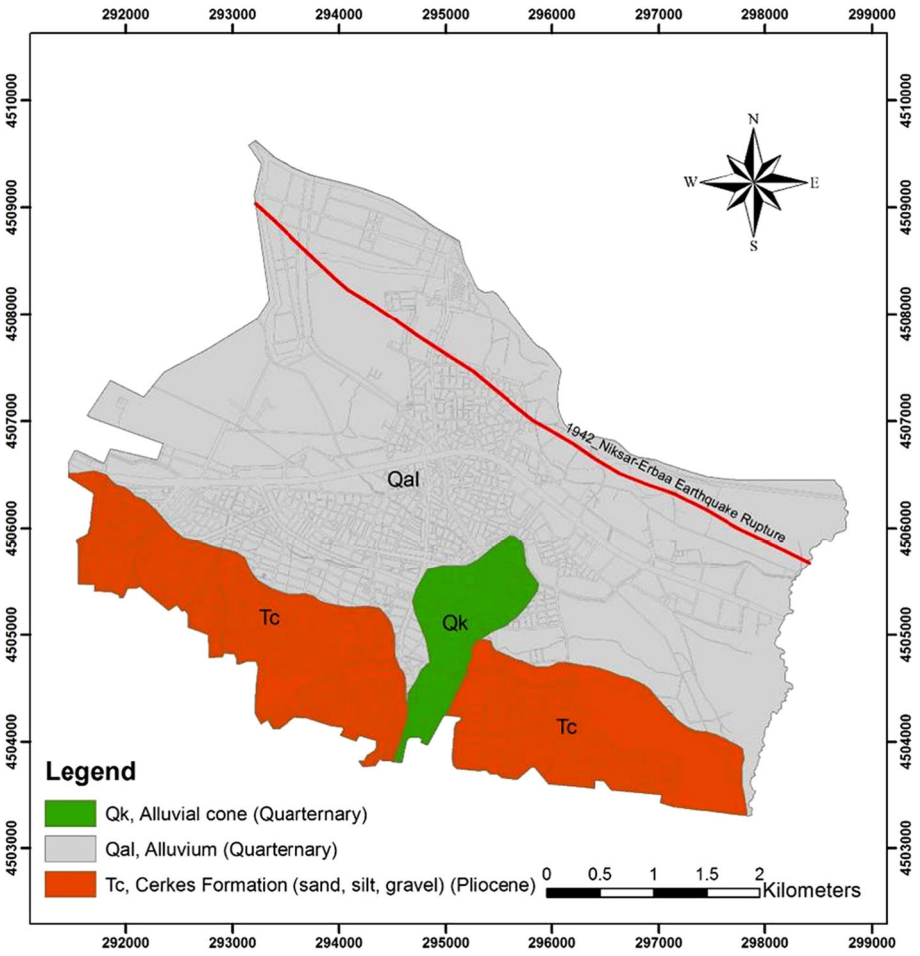

Fig. 3 Geological map of Erbaa

seismic activity with higher magnitude has been recorded since 1942 Erbaa-Niksar earthquake in this region.

3 Subsurface conditions and geotechnical investigations

A total of 104 boreholes were drilled for the geotechnical purposes in the study area. The distribution of the boreholes in this study is shown in Fig. 4. Standard Penetration Tests (SPT) were performed, and undisturbed samples (UD) were taken at 1-m intervals in order to obtain a continuous soil profile as much as possible.

Several geophysical applications were performed at the site to compare the characteristics of soil layers with other field and laboratory studies. Within the context of

geophysical applications, 24 resistivity, 20 seismic refraction, 30 SCPTU applications, and 10 SPT-based uphole surveys were carried out (Fig. 5).

Resistivity surveys were performed at 24 points along 3 profiles in Erbaa to differentiate the subsurface geology and the bedrock depth (Fig. 5). The Schlumberger method was applied during resistivity measurements and a total of 150 m depth was investigated. A low-frequency original resistivity instrument working with an alternative current was employed during the resistivity surveys. A summary of resistivity survey results is given in Table 1. The Pliocene layers can be observed to a depth of approximately 20–25 m below the alluvial layers.

Seismic refraction studies including P and S-wave measurements were performed using a Seistronix brand, 12-channel digital seismograph with 24 byte A/D resolution. Seismic refraction surveys were carried out along three sections in order to determine the thicknesses and shear wave velocities of the soil layers for the site response analyses. Table 2 presents the results of the seismic refraction surveys. S-wave velocities were measured with an average of 202 m/s for the first layer, 341 m/s for the second layer, and 483 m/s for the third layer (Table 2). It is well known that the average shear wave velocity of the uppermost 30 m of the ground (V_{s30}) is an important factor for the site classifications (Borcherdt 1994; Dobry et al. 2000).

A total of 30 SCPTU (seismic cone penetration test with pore pressure measurement) recordings were performed with varying depths in accordance with ASTM D5778-95

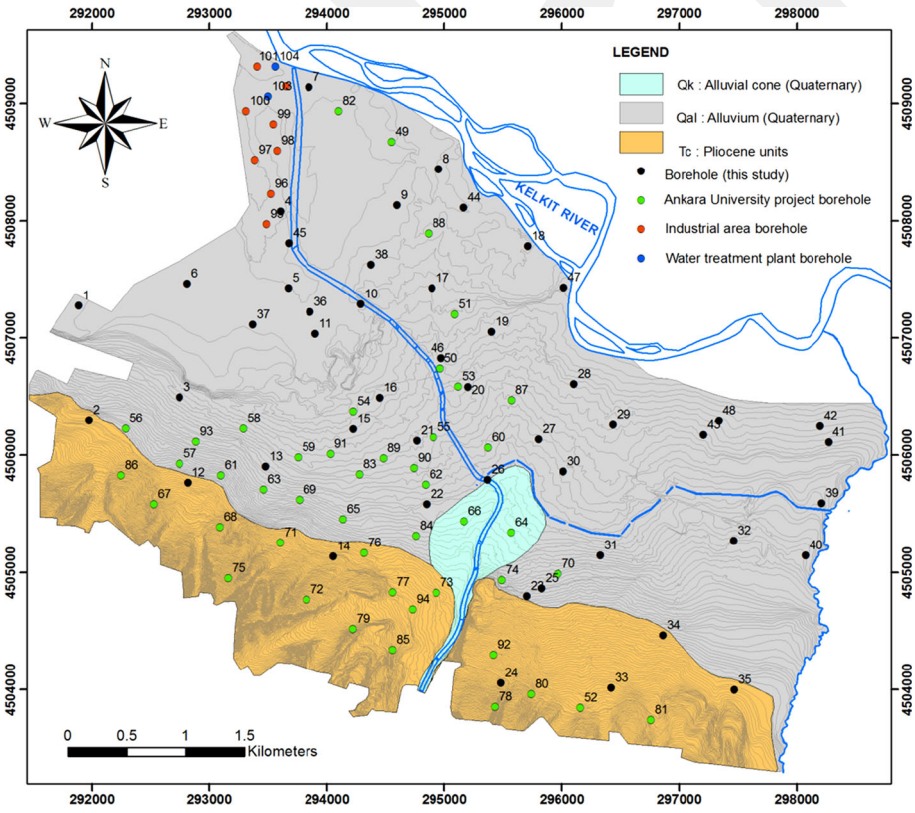

Fig. 4 The general distribution of the boreholes

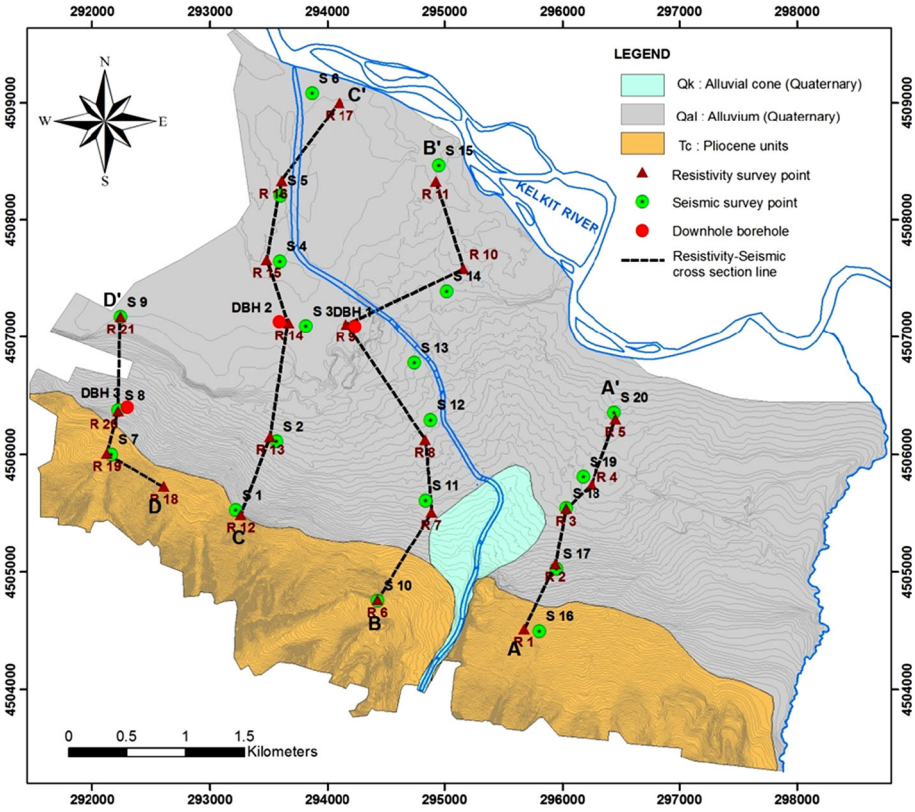

Fig. 5 The location points of geophysical surveys

(2000) standards. The performance of the CPT apparatus was significantly affected by gravelly layers in the study area. Therefore, a limited number of CPT tests could be performed at shallow depths. The minimum and maximum investigation depths were 0.4 and 11.4 m, respectively. An example of SCPTU test result is given in Fig. 6.

The SPT-based uphole surveys that use the impact energy of the split spoon sampler in SPT test as a source was first introduced by Ohta et al. (1978). After Ohta et al. (1978), Kim et al. (2004) and Bang and Kim (2007) used the same method by interpreting the test results. They introduced the SPT-based uphole test as a combination of low and high-strain tests. The SPT-based uphole test is a modified version of the seismic uphole method. Moreover, it is a field seismic test that uses a number of receivers (geophones) inserted on the ground surface to obtain the shear wave velocity (V_s) profile of a site. A schematic diagram of the SPT-based uphole method is shown in Fig. 7. In this method, it is aimed to record the shear waves during SPT test without any additional explosives or mechanical sources. One of the typical examples of SPT-based uphole records is depicted in Fig. 8 for BH-10 (Akin et al. 2011a, b).

The SPT-based uphole method was first used in Turkey as a part of this microzonation study. Consequently, it was applied in 10 drilled boreholes to obtain shear wave velocity profiles. A total of seven geophones spaced at a 2-m interval were placed on the ground surface, and the recordings were made at every 1 m during hammering in SPT applications. As recommended, two-component geophones were preferred in order to obtain better

Table 1 The resistivity survey results

Resistivity location	*X*	*Y*	*Z* (m)	Lithological Unit	Thickness (m)	Apparent resistivity (Ωm)
R-1	4,504,511	295,677	257	Residual soil	7	70
				Gravel	7	50
				Marn-sandstone	–	20
				Marn-sandstone	–	30
				Marn-sandstone	–	30
R-2	4,505,064	295,943	242	Residual soil	10	110
				Gravel	22	65
				Marn-sandstone	–	20
R-3	4,505,545	296,034	213	Residual soil	3	36
				Clay	13	15
				Sand	81	40
				Marn-Sandstone	–	20
R-4	4,505,747	296,253	221	Residual soil	7	70
				Clay	22	18
				Gravel-sand	92	40
				Marn-Sandstone	–	30
R-5	4,506,304	296,460	211	Residual soil	7	65
				Residual soil	7	130
				Gravel-sand	25	50
				Gravel	62	80
				Marn-sandstone	–	20
R-6	4,504,762	294,432	260	Sandy clay	7	50
				Gravel	26	170
				Marn-sandstone	–	15
R-7	4,505,511	294,890	223	Sandy clay	7	30
				Gravel	40	120
				Marn-sandstone	–	12
R-8	4,506,127	294,837	216	Gravel	18	40
				Gravel	41	200
				Gravel	–	70
R-9	4,507,108	294,163	202	Gravel-sand	9	100
				Sand-gravel	50	50
				Marn-sandstone	–	12
R-10	4,507,583	295,161	200	Gravel-sand	10	140
				Gravel	14	60
				Sand-gravel	25	100
				Sand-gravel	–	50
R-11	4,508,327	294,926	202	Gravel-sand	5	85
				Gravel	58	120
				Sand-gravel	–	75

Table 1 continued

Resistivity location	*X*	*Y*	*Z* (m)	Lithological Unit	Thickness (m)	Apparent resistivity (Ωm)
R-12	4,505,490	293,261	243	Residual soil	4	34
				Gravel-sand	4	100
				Marn-sandstone	–	40
R-13	4,506,154	293,511	216	Residual soil	4	30
				Gravel-sand	24	70
				Marn-Sandstone	–	22
R-14	4,507,122	293,668	199	Residual soil	6	18
				Gravel-sand	25	70
				Marn-sandstone	–	22
R-15	4,507,660	293,484	200	Residual soil	2	15
				Gravel-sand	36	60
				Marn-Sandstone	–	20
R-16	4,508,330	293,611	200	Gravel	8	100
				Gravel	62	120
				Sandstone	–	40
R-17	4,509,001	294,102	198	Gravel	8	140
				Gravel	–	130
R-18	4,505,730	292,608	246	Sand-gravel	8	34
				Gravel	28	100
				Marn-sandstone	–	34
R-19	4,506,010	292,127	246	Sand-gravel	19	34
				Gravel	17	100
				Marn-sandstone	20	22
				Marn-sandstone	–	28
R-20	4,506,867	291,522	215	Sand-gravel	6	19
				Sand-gravel	46	44
				Marn-sandstone	–	16
R-21	4,507,178	292,240	196	Sand-gravel	102	25
				Marn-sandstone	–	8

travel time information. Two recordings were conducted at the same depth during SPT application for accurate results (Akın 2009; Akin et al. 2009, 2011a, b, 2013).

4 Site response analyses

One-dimensional site response analyses are based on the assumption that all boundaries are horizontal and the response of a soil deposit is caused by SH-waves propagating vertically from the underlying bedrock. In this study, software called ProSHAKE (v.1.12) (EduPro Civil Systems) is used to perform 1-D equivalent site response analyses. The features of this software are highly compatible and allow evaluating modulus reduction and damping models.

Table 2 The seismic refraction survey results

Seismic refraction survey#	*X*	*Y*	*Z*	Layer 1			Layer 2			Layer 3		
				Depth (m)	V_s–1 (m/s)	V_p–1 (m/s)	Depth (m)	V_s–2 (m/s)	V_p–2 (m/s)	Depth (m)	V_s–3 (m/s)	V_p–3 (m/s)
DBH2												
S1	4,505,531	37,293,219	240	0–1	55	212	1–16	196	590	>16	392	790
S2	4,506,113	37,293,565	215	0–1	110	443	>9	279	887			
S3	45,079,097	37,293,817	198	0–9	138	350				>1	519	1660
S4	4,507,648	37,293,594	197	0–1	80	385				>4	350	1544
S5	4,508,205	37,293,601	192	0–4	143	340				>2	447	1500
S6	4,509,083	37,293,870	193	0–2	87	335				>3	216	1170
S7	4,506,003	37,292,164	246	0–3	373	419				>14	691	1645
DBH3												
S8	4,506,877	37,291,521	217	0–14	352	566				>13	734	1486
S9	4,507,175	37,292,242	198	0–13	292	381				>1	?	1811
S10	4,504,755	37,294,432	263	0–1	254	481				>11	?	1196
S11	4,505,612	37,294,839	223	0–11	294	421	9>	526	824			
S12	4,506,295	37,294,881	192	0–9	228	357	4–10	?	654	>10	?	1201
DBH1												
S13	4,506,780	37,294,742	217	0–4	?	340	10>	350	700			
S14	4,507,393	37,295,019	230	0–10	?	285	10>	306	485			
S15	4,508,462	37,294,953	198	0–4	?	265	4–14	272	595	>14	?	
S16	4,504,497	37,295,805	257	0–2	72	270	2–12	431	616	>12	703	1102
S17	4,505,026	37,295,951	229	0–6	209	435	6–60	352	654			829
S18	4,505,548	37,296,036	226	0–3	158	446	3–12	354	570	>12	460	1229
S19	4,505,815	37,296,181	218	0–10	334	382				>10	460	927
S20	4,506,358	37,296,447	220	0–12	255	452				>12	336	986

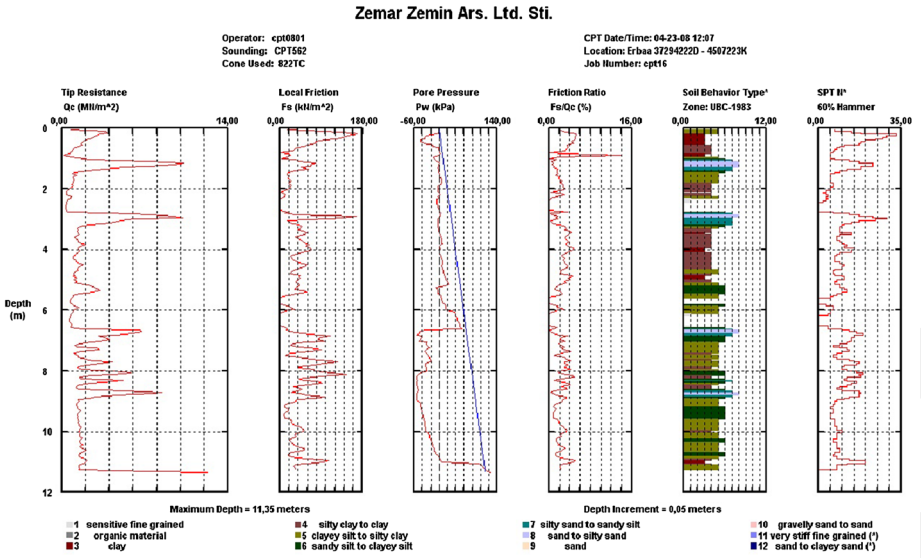

Fig. 6 An example record of SCPTU (CPT-16)

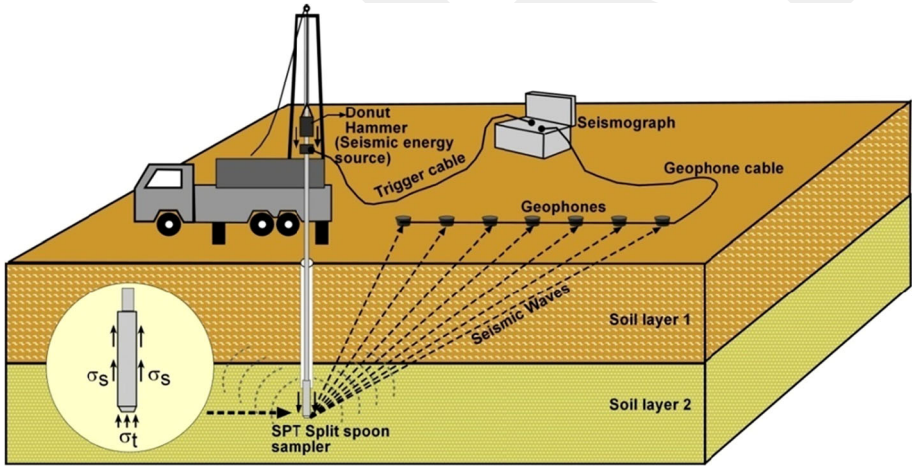

Fig. 7 A schematic diagram of the SPT based uphole method

4.1 Soil parameters used for one-dimensional site response analyses

Dynamic soil parameters including shear wave velocity profiles were prepared for the site response analyses. The shear wave velocities obtained from empirical formulas for different soil types and from SPT-based uphole tests (measured shear wave velocity) are correlated in order to determine the soil profiles of the layers. A series of empirical formulas, which contain SPT-N and V_s relationships proposed by different researchers for the soil types (Ohba and Toriumi 1970; Imai and Yoshimura 1970; etc.), were considered

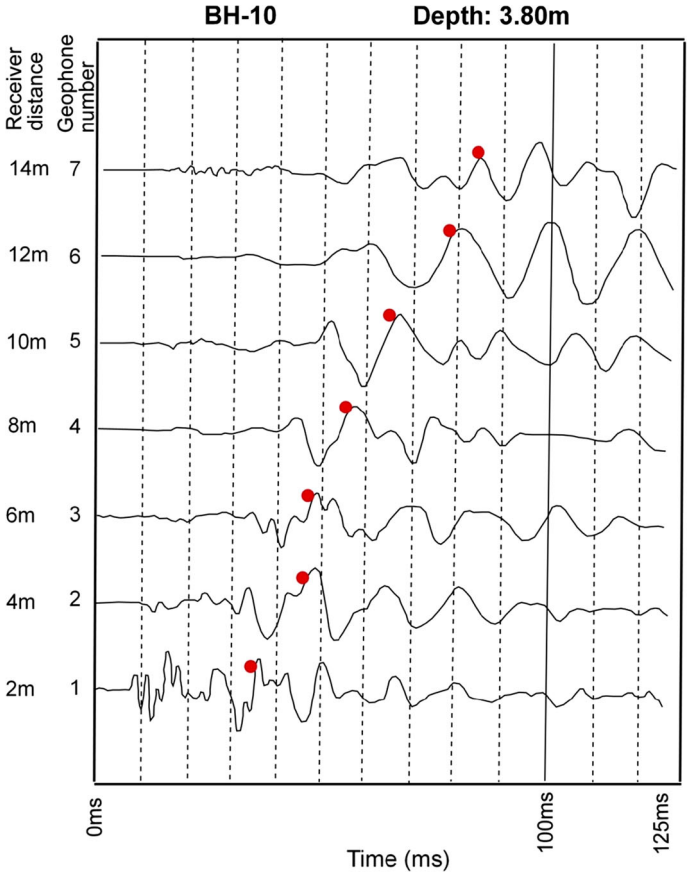

Fig. 8 One of the typical examples of SPT-based uphole records (BH-10)

in this study in order to calculate shear wave velocities. A summary of the empirical relationships between SPT-N and V_s in the literature is presented in Table 3 for different soil types. The SPT-N values obtained from Erbaa soils were then used with these equations to empirically determine a shear wave velocity (V_s) profile for each borehole. Additionally, site-specific SPT-N based V_s relations for Erbaa soil types were also considered in the calculation of shear wave velocity profiles. The energy ratio of SPT is accepted to be 45 % for the equations in this study. The proposed site-specific formulas are given in Table 4.

The geotechnical data from 104 boreholes were evaluated for site response analyses. To allow relatively smooth variation of V_s where appropriate, the shear wave velocity profile for each borehole was defined by generally dividing the soil profile into 3 m (for depth < 100 m) or 5 m (for depth > 100 m) sublayers. Alluvial and Pliocene soil deposits are individually evaluated in four main soil groups: A1-Clay (alluvium clay), A2-Sand (alluvium sand), P1-Clay (Pliocene clay) and P2-Sand (Pliocene sand). The gravelly and silty soil layers were also considered. Instead of using default models, the essential modulus reduction and damping curves were calculated to model the soil units in the study area.

Table 3 Summary of empirical correlations based on SPT-N versus V_s

Researcher (s)	V_s (m/s)		
	All soils	Sands	Clays
Kanai (1966)	$V_s = 19\ N^{0.6}$	–	–
Imai and Yoshimura (1970)	$V_s = 76\ N^{0.33}$	–	–
Ohba and Toriumi (1970)	$V_s = 84\ N^{0.31}$	–	–
Fujiwara (1972)	$V_s = 92.1\ N^{0.337}$	–	–
Shibata (1970)	–	$V_s = 32\ N^{0.5}$	–
Ohta et al. (1972)	–	$V_s = 87\ N^{0.36}$	–
Ohsaki and Iwasaki (1973)	$V_s = 81.4\ N^{0.39}$	$V_s = 59.4\ N^{0.47}$	–
Imai et al. (1975)	$V_s = 89.9\ N^{0.341}$	–	–
Imai (1977)	$V_s = 91\ N^{0.337}$	$V_s = 80.6\ N^{0.331}$	$V_s = 102\ N^{0.292}$
Ohta and Goto (1978)	$V_s = 85.35\ N^{0.348}$	–	–
Seed and Idriss (1981)	$V_s = 61.4\ N^{0.5}$	–	–
Imai and Tonouchi (1982)	$V_s = 97\ N^{0.314}$	–	–
Seed et al. (1983)	–	$V_s = 56.4\ N^{0.5}$	–
Sykora and Stokoe (1983)	–	$V_s = 100.5\ N^{0.29}$	–
Tonouchi et al. (1983)	$V_s = 97\ N^{0.314}$	–	–
Fumal and Tinsley (1985)	–	$V_s = 152 + 5.1\ N^{0.27}$	–
Jinan (1987)	$V_s = 116.1\ (N + 0.3185)^{0.202}$	–	–
Okamoto et al. (1989)	–	$V_s = 125\ N^{0.3}$	–
Lee (1990)	–	$V_s = 57\ N^{0.49}$	$V_s = 114\ N^{0.31}$
Yokota et al. (1991)*	$V_s = 121\ N^{0.27}$	–	–
Kalteziotis et al. (1992)	$V_s = 76.2\ N^{0.24}$	–	–
Pitilakis et al. (1992)	–	$V_s = 162\ N^{0.17}$	–
Athanasopoulos (1995)	$V_s = 107.6\ N^{0.36}$	–	–
Raptakis et al. (1995)	–	$V_s = 100\ N^{0.24}$	–
Sisman (1995)	$V_s = 32.8\ N^{0.51}$	–	–
Iyisan (1996)	$V_s = 51.5\ N^{0.516}$	–	–
Kayabali (1996)	–	$V_s = 175 + (3.75\ N)$	–
Jafari et al. (1997)	$V_s = 22\ N^{0.85}$	–	–
Pitilakis et al. (1999)	–	$V_s = 145(N_{60})^{0.178}$	$V_s = 132(N_{60})^{0.271}$
Kiku et al. (2001)	$V_s = 68.3\ N^{0.292}$	–	–
Jafari et al. (2002)	–	–	$V_s = 27\ N^{0.73}$
Hasançebi and Ulusay (2007)	$V_s = 90\ N^{0.308}$	$V_s = 90.82\ N^{0.319}$	$V_s = 97.89\ N^{0.269}$
Hanumantharao and Ramana (2008)	$V_s = 82.6\ N^{0.43}$	$V_s = 79\ N^{0.434}$	–
Dikmen (2009)	$V_s = 58\ N^{0.39}$	$V_s = 73\ N^{0.33}$	$V_s = 44\ N^{0.48}$

Proper modulus reduction and damping curves for one-dimensional equivalent site response analyses were established using the Darendeli model (Darendeli 2001) in this study. For that reason, the model was re-formulated with different confining pressures to produce curves similar to the EPRI (Electric Power Research Institute 1993) curves. So, site-specific soil models with modified G/G_{max}-shear strain curves were used for the four

Table 4 The proposed site-specific formulas based on SPT N versus V_s

Relationship*	Soil type	r
$V_s = 59.44\ N^{0.109}\ z^{0.426}$	All alluvial soils	0.89
$V_s = 38.55\ N^{0.176}\ z^{0.481}$	Alluvial sand	0.94
$V_s = 78.10\ N^{0.116}\ z^{0.350}$	Alluvial clay	0.92
$V_s = 121.75\ N^{0.101}\ z^{0.216}$	All Pliocene soils	0.94
$V_s = 52.04\ N^{0.359}\ z^{0.177}$	Pliocene sand	0.98
$V_s = 140.61\ N^{0.049}\ z^{0.232}$	Pliocene clay	0.89

* N refers to raw SPT-N value

Table 5 Depth ranges for dynamic curves and the representative depth (EPRI 1993)

Depth range (ft)	Depth range (m)	Representative depth (m)
0–20	0–6	3
20–50	6–12	9
50–120	12–25	18.5
120–250	25–50	32.5
250–500	50–100	75
500–750	100–200	150
>750	>200	>250

previously defined soil groups (A1-Clay, A2-Sand, P1-Clay, and P2-Sand) in this study. The representative depths (in meters) mentioned in Table 5 were taken into consideration during the calculations to reflect different confining pressures. The modified curves are illustrated in Figs. 9, 10, 11, and 12. In these figures, the symbol of each curve (e.g. G/Gmax-strain_3) indicates the representative depth in meters (e.g., 3 m) and the related confining pressure for the same depth. The default curves are also used for gravel, silt, and bedrock layers as defined in ProSHAKE (v.1.12) program. Furthermore, the average unit weight of the soil layers are determined from laboratory test results.

4.2 Modeling of soil profiles for site response analyses

Dividing a study area into grid cells is a common approach used in seismic microzonation applications. The dimension of cells depends primarily upon the availability of geological, geophysical and geotechnical data. The most common grid sizes in the literature are 500 m × 500 m or 250 m × 250 m. Site characterization can be performed based on grid system using the available data for each cell by some authors (Matsuoka et al. 2006; Erdik et al. 2005; Ansal et al. 2006; Ansal and Tonuk 2007).

The study area, Erbaa settlement, was divided into a total of 118, 500 m × 500 m grid cells and seismic response analysis was performed for each cell (Fig. 13). Based on these grid cell areas, the representative soil profiles were statistically extrapolated for the entire study area.

The bedrock profiles were characterized as having constant shear wave velocity ($V_s = 760$ m/s). Ansal and Tonuk (2007) mentioned that the shear wave velocity profiles should be established down to the depth of engineering bedrock with an estimated shear wave velocity of 700–750 m/s. However, the boundary between NEHRP site classes B and C starts with 760 m/s, so that boundary value was accepted as the bedrock shear wave velocity in Erbaa.

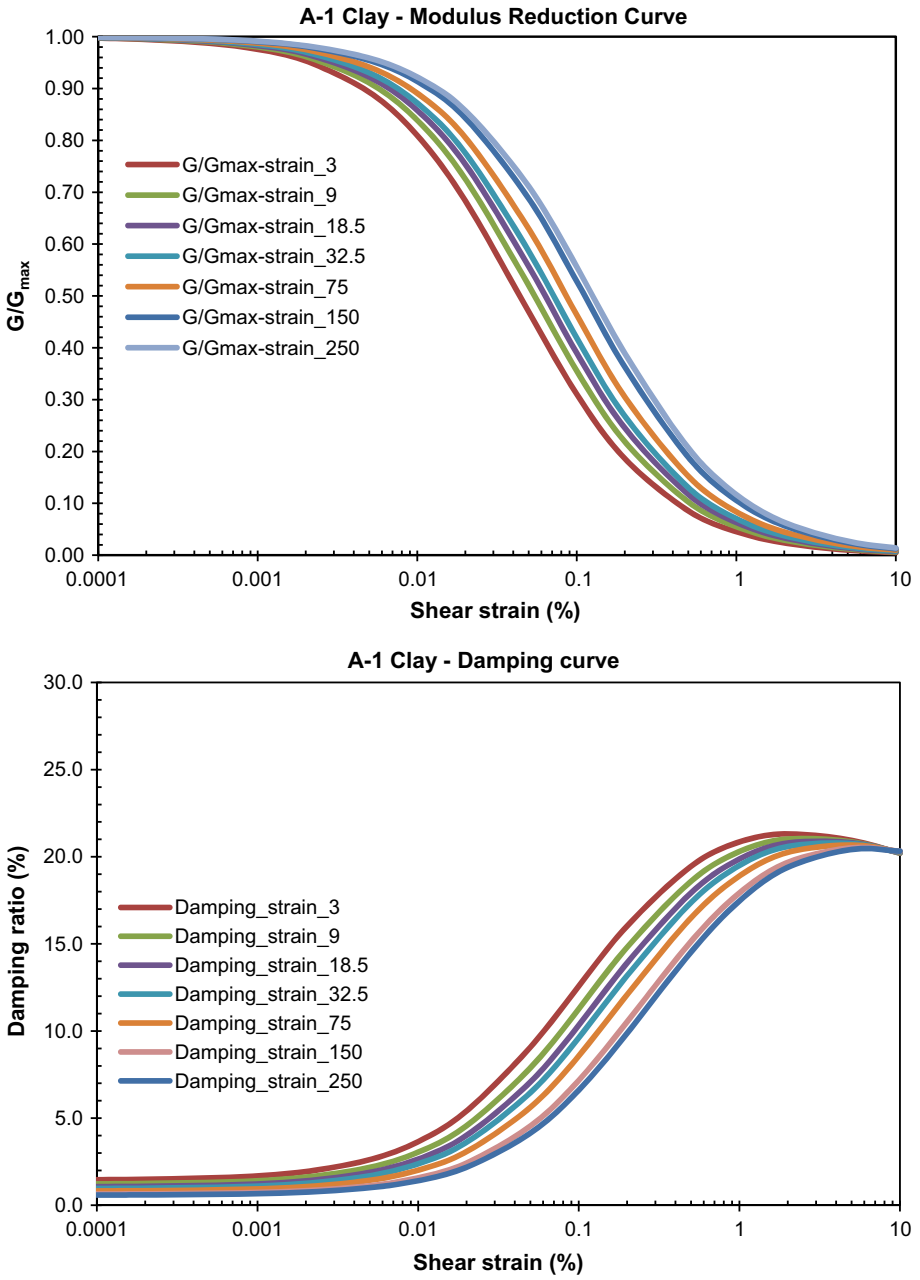

Fig. 9 Modified modulus reduction and damping curves for alluvium clay (A-1)

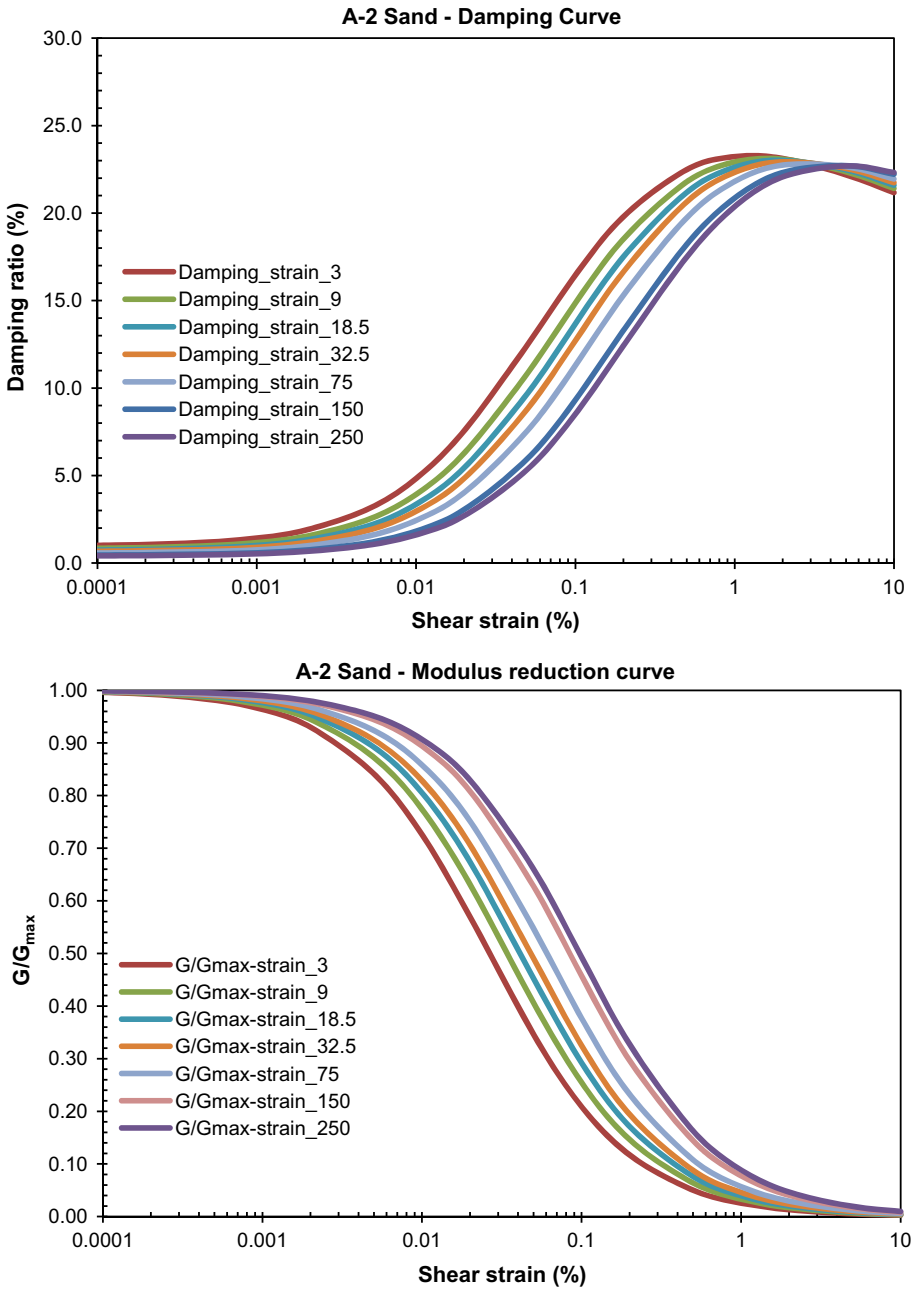

Fig. 10 Modified modulus reduction and damping curves for alluvium sand (A-2)

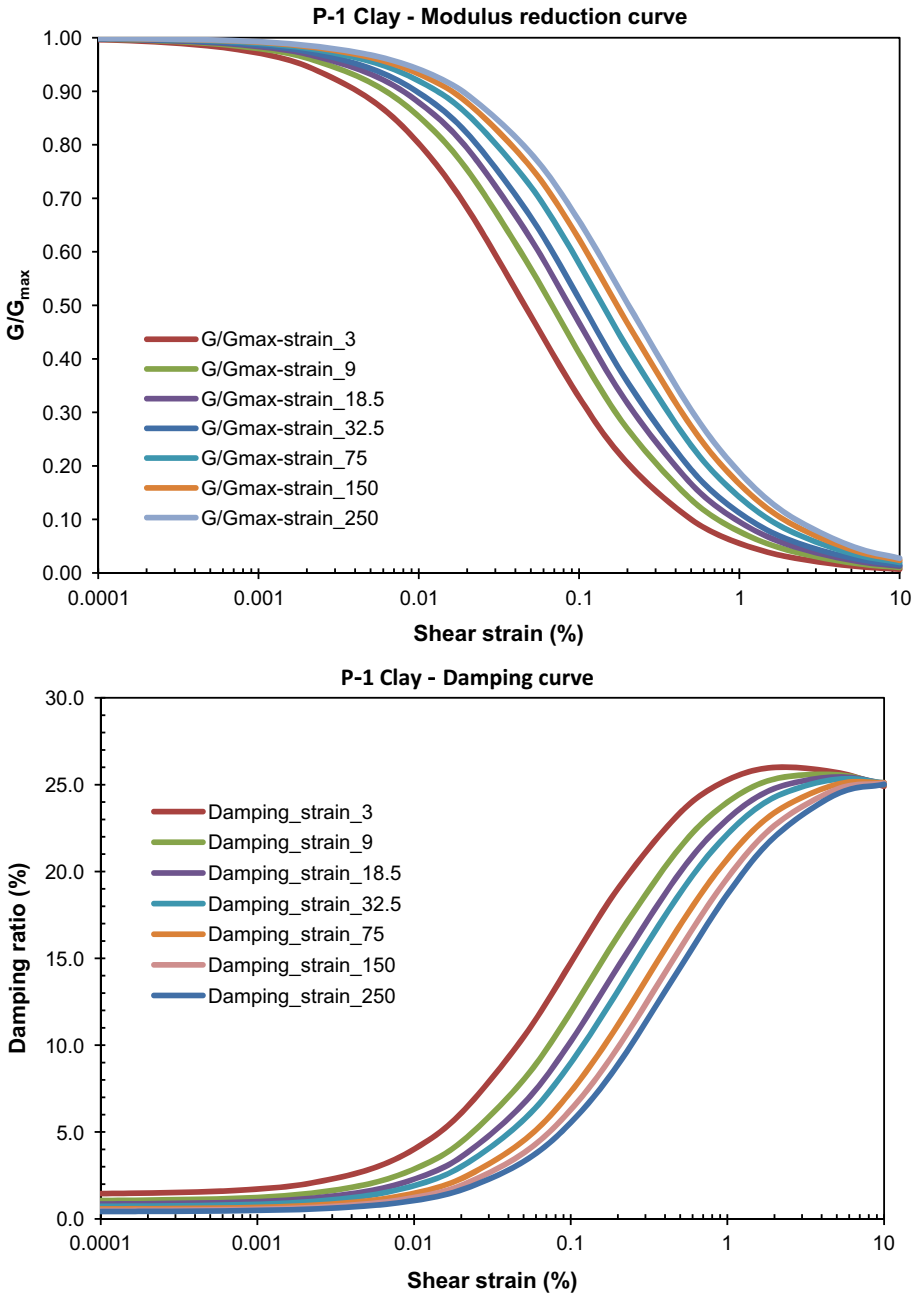

Fig. 11 Modified modulus reduction and damping curves for Pliocene clay (P-1)

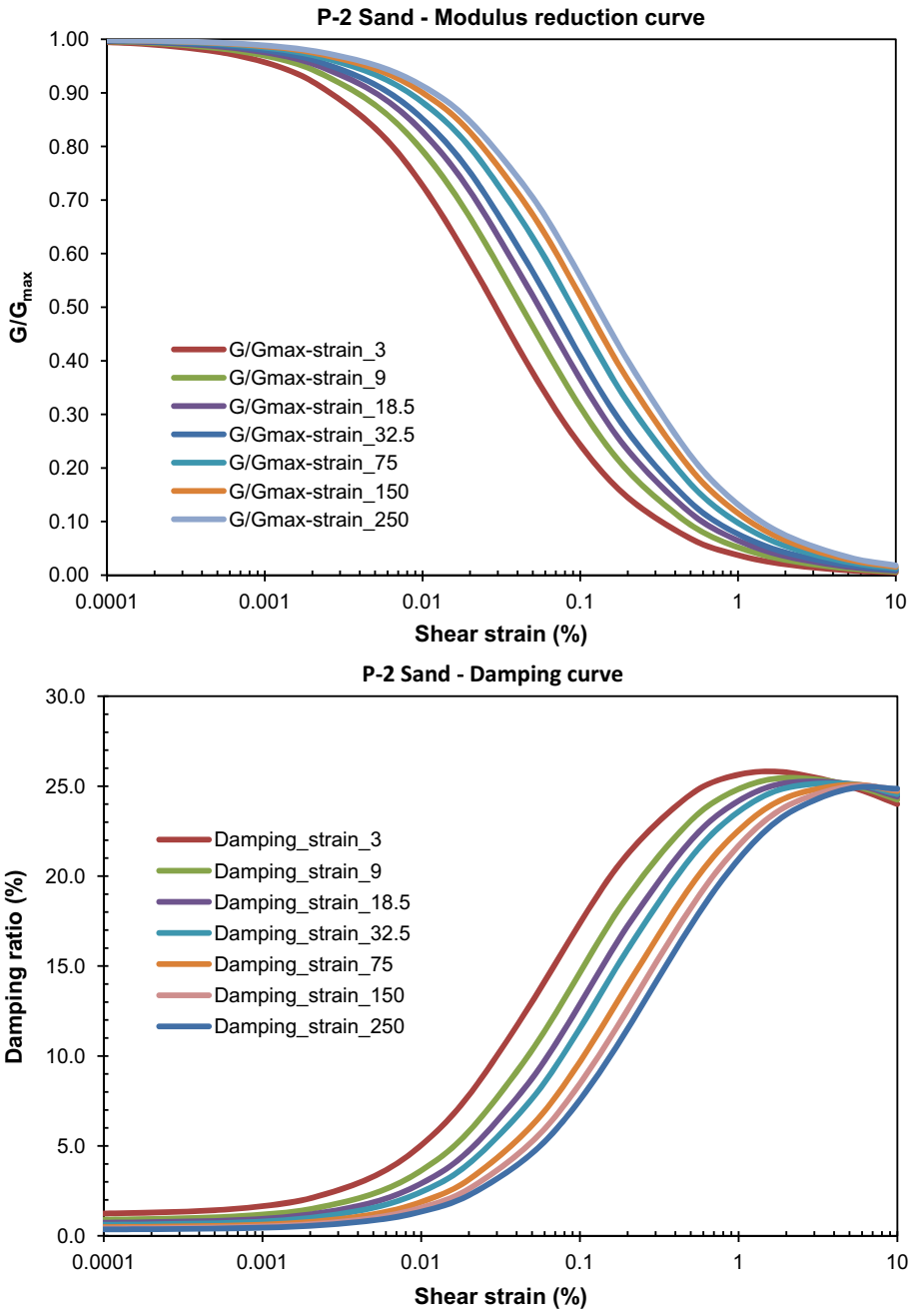

Fig. 12 Modified modulus reduction and damping curves for Pliocene sand (P-2)

The soil profiles are extended using the power-law relationships given in Table 4 to the depth where the shear wave velocity is 760 m/s for boreholes in which shear wave velocities for rock units are unavailable (Akın 2009). The available data for each cell is

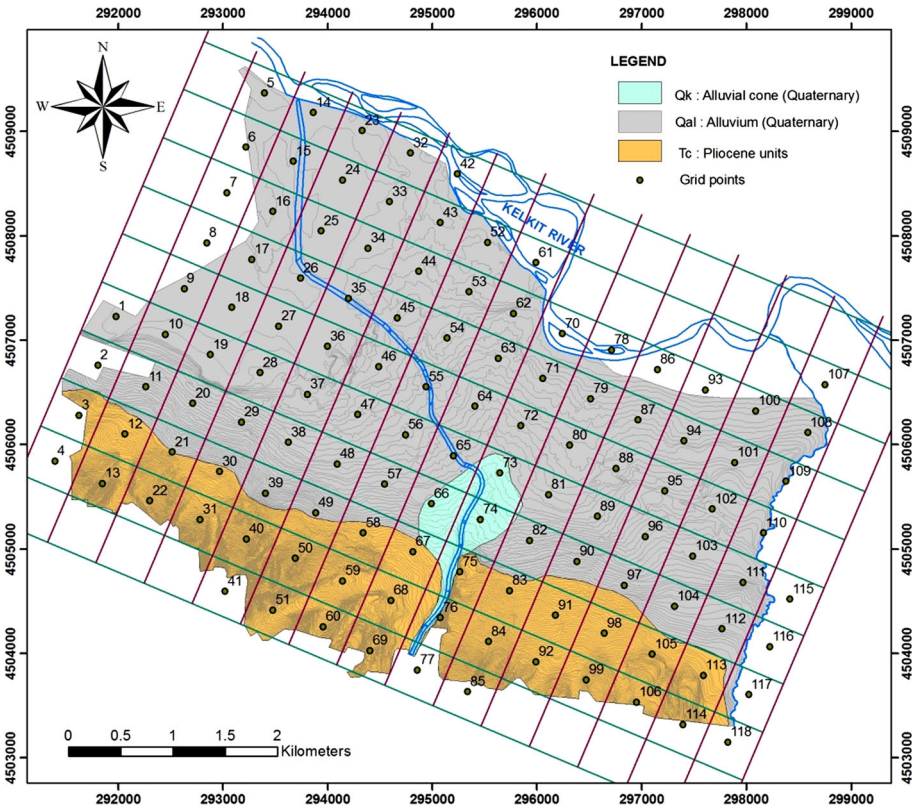

Fig. 13 Grid system used for site response analysis

used in site response analysis. For empty cell or unavailable data conditions, the nearest borehole data were used to perform the site response analysis (Akın 2009).

4.3 Ground motions used for site response analyses

An earthquake magnitude of 7.2 from 0 to 4 km rupture distances is accepted for the regional earthquake hazard analysis (Akın 2009). Scaled acceleration time histories are selected on the basis of the best match to target spectra obtained from Next Generation Attenuation (NGA) ground motion models. In total, 14 (seven for Boore and Atkinson (2008) and seven for Campbell and Bozorgnia (2008) NGA relationships) scaled acceleration time histories were defined for each cell. These 14 ground motions were used as input motions in the site response analyses (Table 6). An example of one of the ground motions is shown in Fig. 14. During the analyses, the essential scaled peak ground acceleration (PGA) values (given in Table 7) are assigned for each analysis point.

The proposed soil profiles and ground motions are used as inputs for the site response analyses using ProSHAKE software. The input motions are assigned in the input motion section of the software. Additionally, it is possible to obtain response spectrum for each motion to be used in amplification ratio analyses.

Table 6 Strong ground motion input data used in this study

Associated number in this study	Earthquake name	Location	Year	Magnitude	ClstD (km)	PGA (g)	PGV (cm/s)	PGD (cm)
9	Imperial Valley-06	Imperial Valley-06, El Centro Array#11	1979	6.5	12.5	0.37	38.4	17.7
10	Imperial Valley-06	Imperial Valley-06, El Centro Array#3	1979	6.5	12.9	0.26	40.8	21.0
16	Imperial Valley-06	Imperial Valley-06, El Centro Differential Array	1979	6.5	5.1	0.43	55.3	33.0
19	Irpinia, Italy-01	Irpinia, Italy-01, Sturno	1980	6.9	10.8	0.29	46.9	21.5
34	Loma Prieta	Loma Prieta, Saratoga–Aloha Ave	1989	6.9	8.5	0.38	48.5	20.3
40	Kobe, Japan	Kobe, Japan, Takarazuka	1995	6.9	0.3	0.71	75.9	23.1
42	Kocaeli, Turkey	Kocaeli, Turkey, Gebze	1999	7.5	10.9	0.18	38.3	33.7

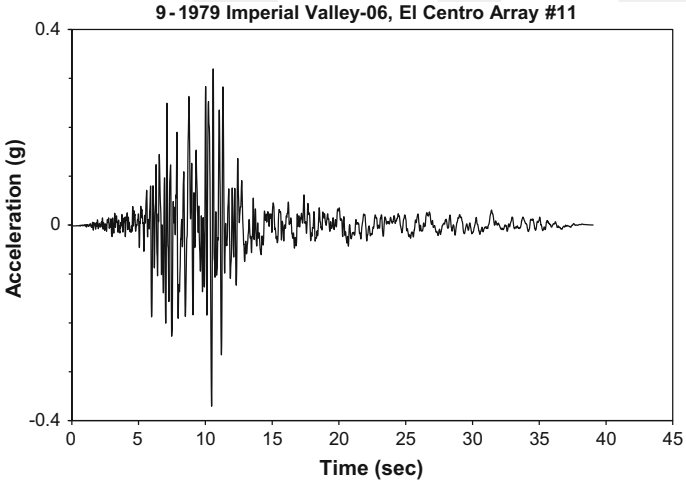

Fig. 14 Time history of ground motion 9

5 Assessments on site amplification

5.1 Amplification obtained from 1-D linear equivalent site response analyses

Time histories obtained from ground response analyses can be used directly to represent ground surface motions, synthetic time-histories can be developed to match the design ground surface response spectrum (U.S. Army Corps of Engineers 1999), or recorded motions can be scaled or modified to match some desired target spectrum. The direct use of response spectra from the calculated surface motions is generally not preferred in

Table 7 Distance-dependent PGA values for different earthquake ground motions

Ground motion no	Peak ground acceleration					
	Boore and Atkinson (2008)			Campbell and Bozorgnia (2008)		
	0 km	2 km	4 km	0 km	2 km	4 km
9	0.4076	0.3486	0.2754	0.3519	0.3297	0.2892
10	0.4522	0.3754	0.3016	0.3774	0.3543	0.3208
16	0.4332	0.3713	0.2911	0.3434	0.3493	0.3023
19	0.4464	0.3799	0.2984	0.3713	0.3508	0.3145
34	0.4827	0.4003	0.3201	0.4021	0.3836	0.3379
40	0.4669	0.4007	0.3133	0.4000	0.3973	0.3296
42	0.4505	0.4587	0.3556	0.4430	0.4242	0.3811

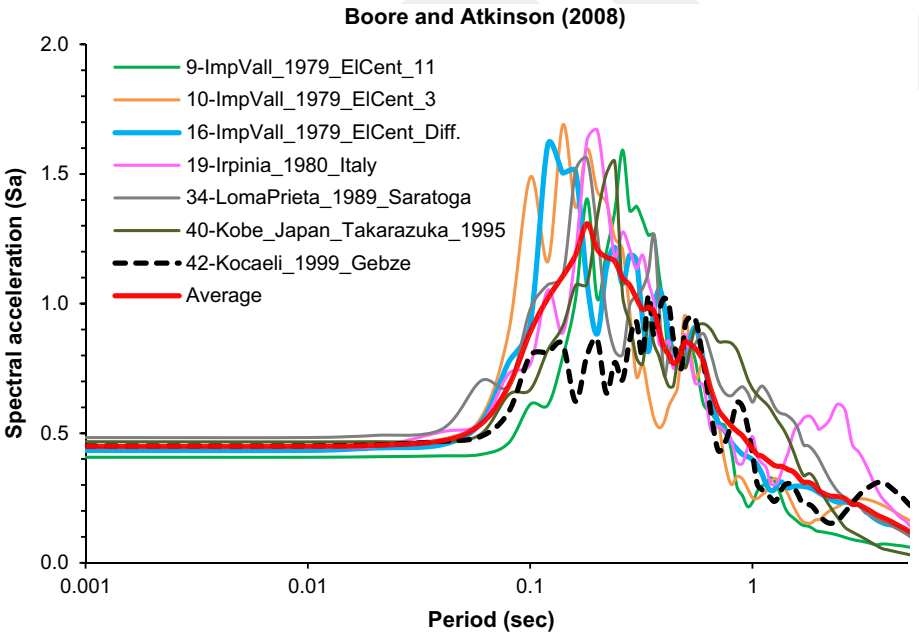

Fig. 15 Input response spectra of BH-4 based on Boore and Atkinson (2008) model for 0-km-distance zone

practice. However, it is advantageous to obtain site amplification ratio from the ground response analyses. The site amplification factor is the ratio between equivalent measures of ground surface motion intensity and the intensity of corresponding input rock motions, i.e.,

$$AF = \frac{IM\ \text{soil}}{IM\ \text{rock}} \tag{1}$$

where *IM* is the intensity measure.

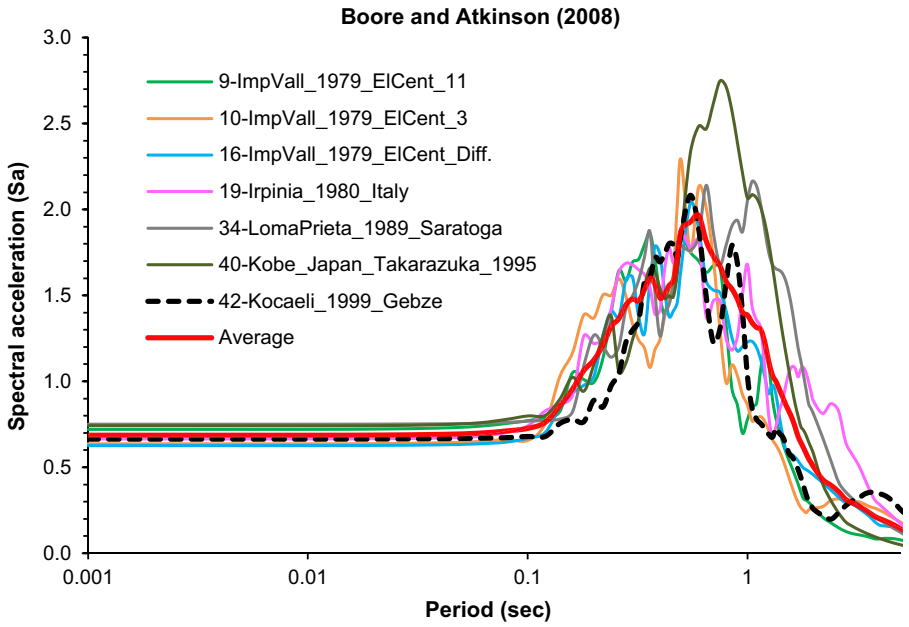

Fig. 16 Surface response spectra of BH-4 based on Boore and Atkinson (2008) model for 0-km-distance zone

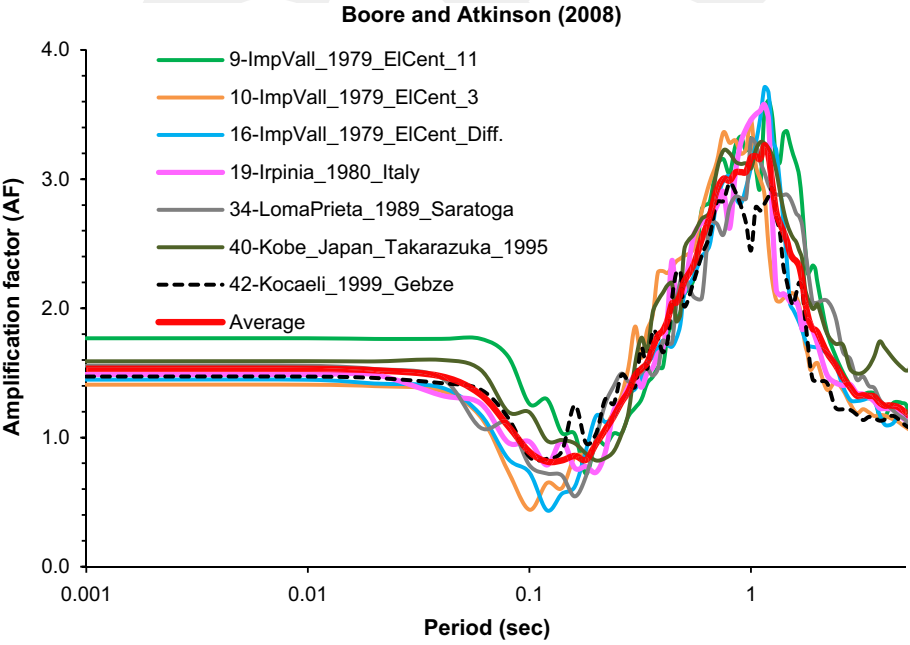

Fig. 17 Amplification ratio of BH-4 based on Boore and Atkinson (2008) model for 0-km-distance zone

Table 8 Results of site response analysis for BH-4

Ground motion	Maximum surface PGA (g)		BA08 model		CB08 model	
	BA08 model	CB08 model	Amplification ratio (AF) (for PGA)	Predominant period (ss) (from ProSHAKE)	Amplification ratio (AF) (for PGA)	Predominant period (s) (from ProSHAKE)
9	0.721	0.676	1.8	1.21	1.9	1.21
10	0.637	0.559	1.4	0.99	1.5	0.99
16	0.627	0.536	1.4	1.28	1.6	0.95
19	0.664	0.596	1.5	0.97	1.6	0.97
34	0.751	0.659	1.5	1.24	1.6	1.24
40	0.741	0.656	1.6	0.87	1.7	0.87
42	0.663	0.687	1.5	1.15	1.5	1.15
Average	0.686	0.624	1.5	1.10	1.6	1.05

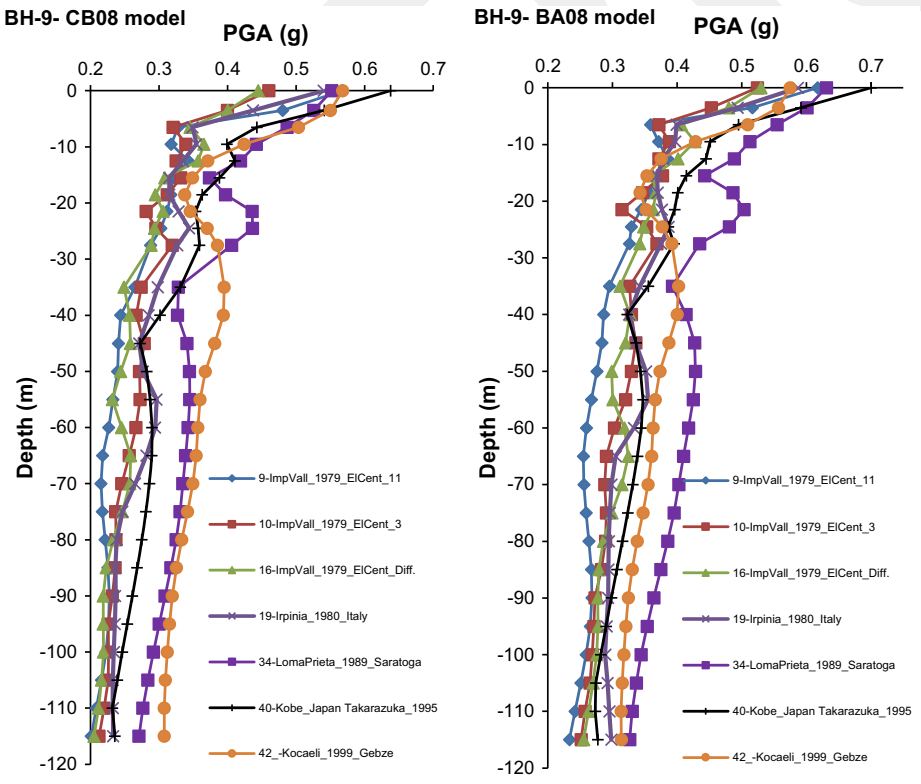

Fig. 18 Variation of PGA values along depth for alluvium units in BH-9

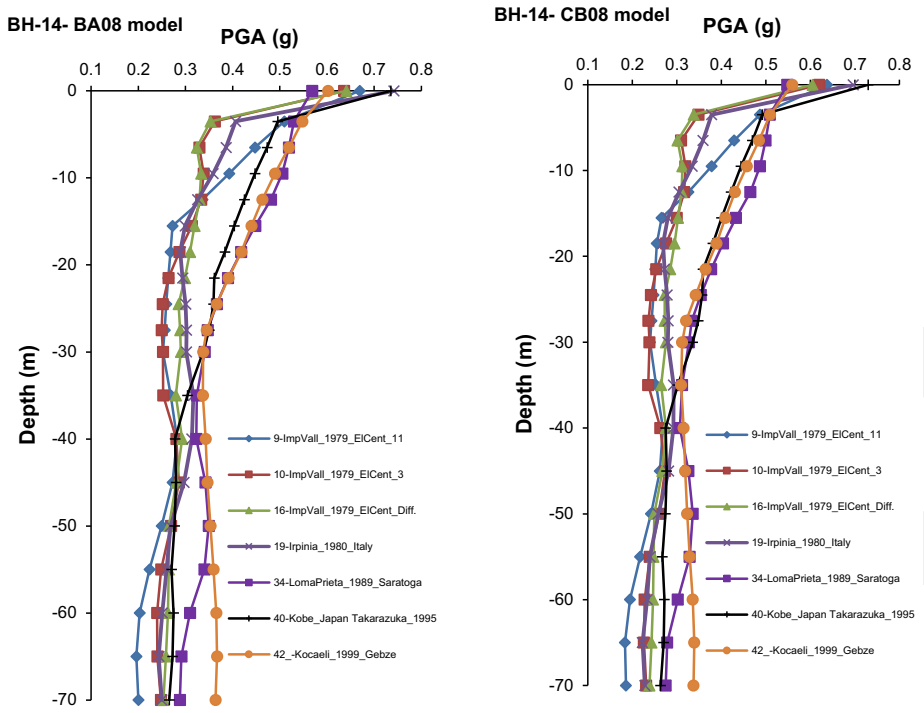

Fig. 19 Variation of PGA values along depth for Pliocene units in BH-14

In the site response analyses of Erbaa, input ground motions were characterized using the PGA values given in Table 7. Afterward, amplification factors based on spectral accelerations were calculated using soil/bedrock ratio (Borcherdt 1970) as given in Eq. 2 to obtain spectral acceleration amplification factors for the study area.

$$AF(T) = \frac{Sa\,\text{soil}\ (T)}{Sa\,\text{rock}\ (T)} \tag{2}$$

The distribution of the selected input ground motions is depicted for BH-4 representing the response spectra of the used ground motions for 5 % damping as given in Fig. 15. The surface time histories obtained from the site response analyses are illustrated in Fig. 16. The calculated amplification factors are also shown in Fig. 17 with respect to Boore and Atkinson (2008) (BA08) model, which has been introduced that the input motions are scaled to be compatible with BA08 model. It should be noted that different distance zones are also considered during the site response analysis.

A summary of data obtained from the ProSHAKE (v.1.12) analyses for the soil profile BH-4 is given as an example in Table 8 including both the NGA models. As seen in Table 8, the surface peak ground acceleration varies between 0.53 and 0.75 g for different earthquakes in BH-4. Besides, the predominant periods range between 0.8 and 1.2 s. The amplification ratios are mostly around 1.5 for both NGA models. The results obtained from

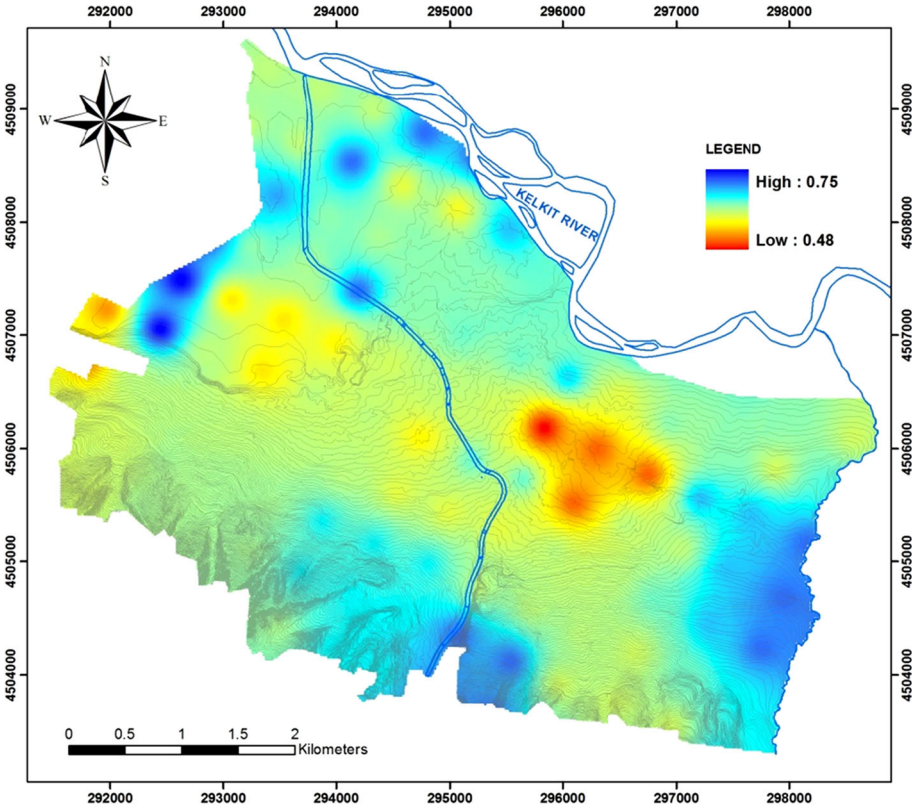

Fig. 20 Peak ground acceleration (PGA) (surface) map of the study area based on Boore and Atkinson (2008) model

both NGA-based models reveal that the amplification factors based on BA08 model are slightly less than the factors based on CB08 model. The slight difference can be explained by the consideration of different model parameters. For instance, in the application of the NGA model calculations, BA08 model considers the closest horizontal distance to the surface projection of the rupture plane (R_{JB}). However, CB08 model uses the closest distance to the rupture plane (R_{rup}). Although there is a slight difference in amplification factors, the PGA values of BA08 model are generally higher than those of CB08 model.

The variation of the PGA values with depth for different earthquake motions and attenuation models is illustrated in Figs. 18 and 19 for the alluvium (BH-9) and the Pliocene (BH-14) units.

The peak ground acceleration (PGA) from the surface motions and amplification maps are prepared using the obtained data from the site response analysis based on the aforementioned 118 grid points in the grid system (Figs. 20, 21, 22, 23). Moreover, the predominant periods obtained from ProSHAKE results are also spatially illustrated in Figs. 24 and 25 for BA08 and CB08 models.

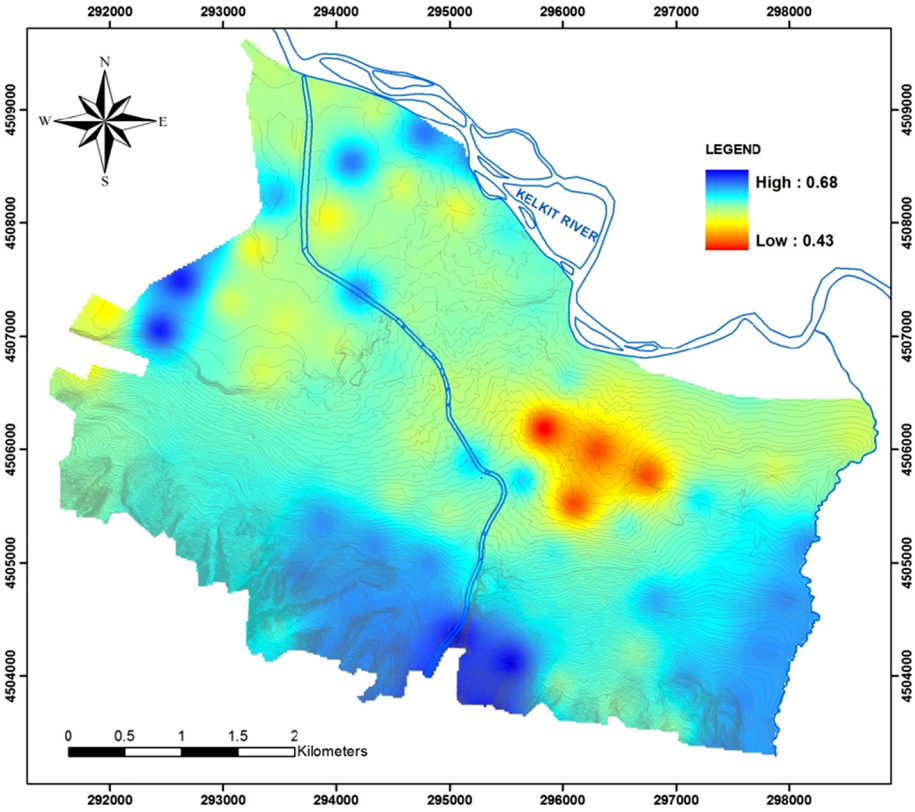

Fig. 21 Peak ground acceleration (PGA) (surface) map of the study area based on Campbell and Bozorgnia (2008) model

The predominant period varies between 0.48 and 1.85 s in the study area. The soil units along the Kelkit River generally exhibit a period range of 0.96–1.23 s. The Pliocene soil layers relatively have low periods (high frequencies) around 0.48–0.76 s. The highest predominant period is found in the central part of Erbaa in the alluvial units where the soil layers are likely to be thickest. The amplification values are quite similar for both NGA-based models. Furthermore, high amplification values for longer periods (more than 3.5) are locally observed along the Kelkit River embankment.

5.2 Amplification obtained from shear wave velocity empirical approaches

Shear wave velocity of soil layers can also be used for the evaluation of the ground amplification. There are a number of shear wave velocity-based amplification formulas in the literature (Midorikawa 1987; Joyner and Fumal 1984; Borcherdt 1994). The proposed equations were also evaluated in TCEGE (1999), and an assessment was made showing the comparison of relative amplification factors determined by the equations presented in Table 9.

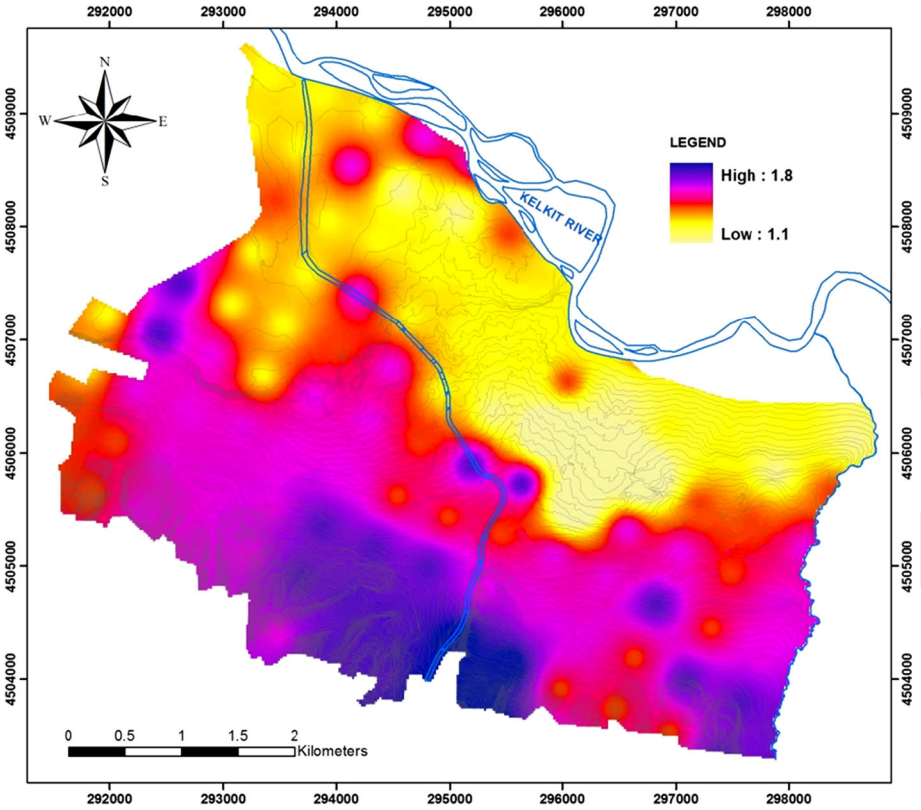

Fig. 22 Amplification map of the study area based on Boore and Atkinson (2008) model (for 0.001 s)

The equation proposed by Midorikawa (1987) was used for the determination of amplification factors in the study area. The previously and newly developed empirical formula-based V_{s30} values for Erbaa were used for the calculation of V_s-based amplification factors (Akın 2009). The amplification results for each borehole are summarized in Table 10.

As seen in the related table, the amplification factors range between 1.92 and 2.88 for different boreholes. The mean amplification factor for the study area is found to be 2.34 considering all soil profiles. Furthermore, the mean amplification factors for alluvial and Pliocene soils are 2.38 and 2.17, respectively. The distribution of amplification factors based on the Midorikawa (1987) shear wave velocity approach is illustrated in Fig. 26.

The lowest amplification factors are generally observed in Pliocene soil layers in accordance with the Midorikawa (1987) approach. Amplification factors were also found to increase toward the northwestern part of the study area in the alluvial layers near the Kelkit River.

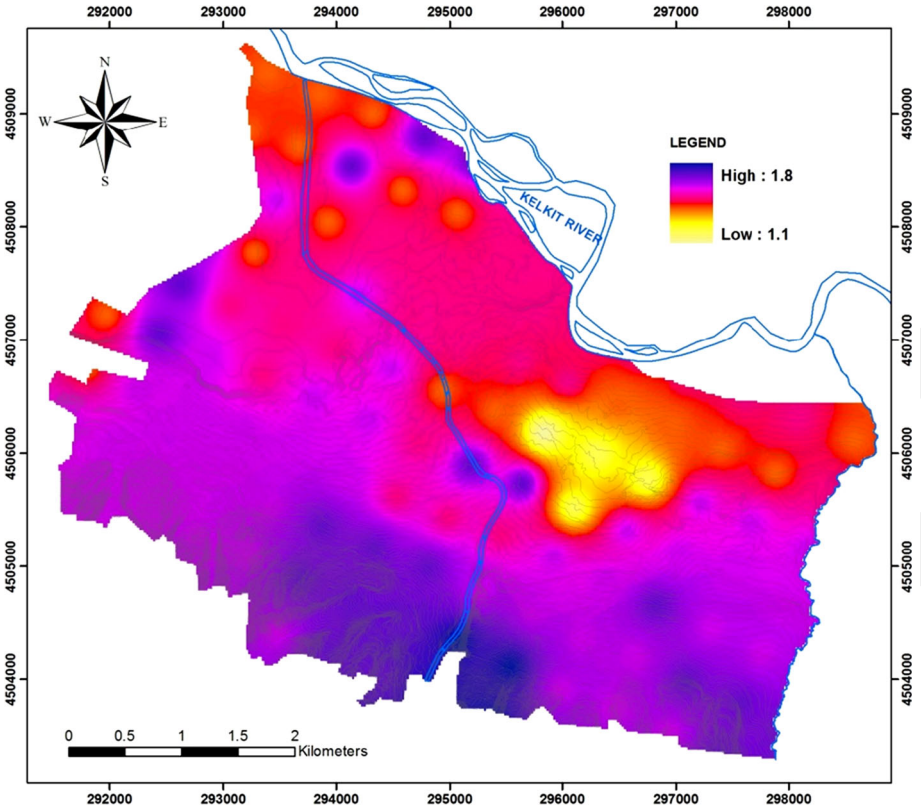

Fig. 23 Amplification map of the study area based on Campbell and Bozorgnia (2008) model (for 0.001 s)

6 Comparison of site amplifications based on two approaches

Seismic hazards during many disastrous earthquakes are observed in the sites with the soil deposits due to amplification of ground motion as referred in the previous sections. In this paper, seismic site response analysis that involves the propagation of earthquake ground motions through the soil layers to the ground surface near fault geometry is highly considered. Due to the lack of the records of strong ground motion of this location, the ground motions having similar properties with this area were used during site response analyses.

The influence of the alluvial units of a site on the seismic response of structures is sometimes higher due to a resonance effect when the predominant periods of the structures and site periods are close to each other. The amplification at sites with these type of soil deposits is larger and longer than that compared with the shaking experienced at a hard rock site (Borcherdt 1994).

The site amplifications and predominant site periods obtained from the above-mentioned two methods (1-D dynamic site response analyses-based and V_s-based empirical approach) are compared in the following paragraphs for this seismically active area. The compared results are summarized in Table 11 depending on the maximum, minimum, and

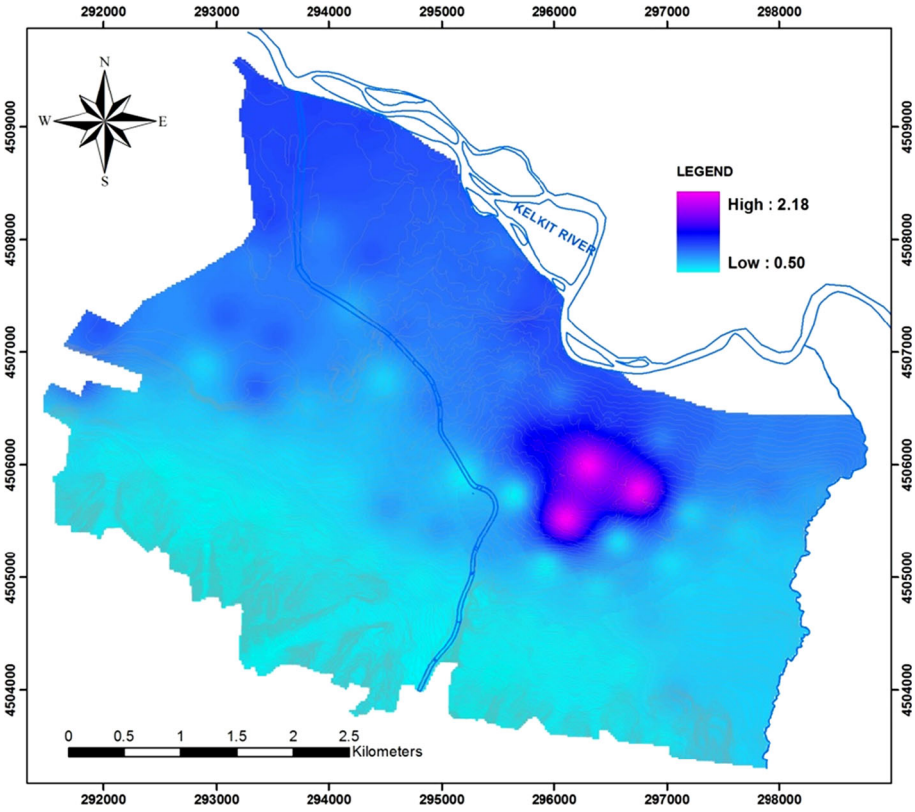

Fig. 24 Predominant period map of the study area (for BA08 model)

mean values of each parameter. Moreover, the amplification factors are compared for each borehole. Afterward, the produced maps from the amplification factors obtained from V_s-based empirical equations (Midorikawa 1987), and the amplification factors obtained from 1-D dynamic site response analyses (ProSHAKE (v.1.12) analyses) are compared to provide the differences of amplification values. There is a significant discrepancy between linear and V_s-based methods with regard to the applied parameters. During site response analyses, amplification factors mostly depend on the raw SPT-N value in V_s based methods. However, 1-D equivalent linear site response analyses consider different parameters.

The general trend of amplification values that covers most of the study area varies between 0.49 and 2.18. High amplification values can be expected in the alluvial units in the study area in accordance with two different models (BA08 model and CB08 model). Moreover, when the predominant periods obtained from ProSHAKE analyses are considered, it can be seen that the predominant periods from the site response analyses are smaller in the Pliocene layers than in the alluvial soils. As a result, 1-D site response analyses reveal reasonable results considering the soil characteristics of the study area. It reveals that procedures based on 1-D ground response analyses which are shown to predict ground responses in reasonable agreement with measured responses as given in this study.

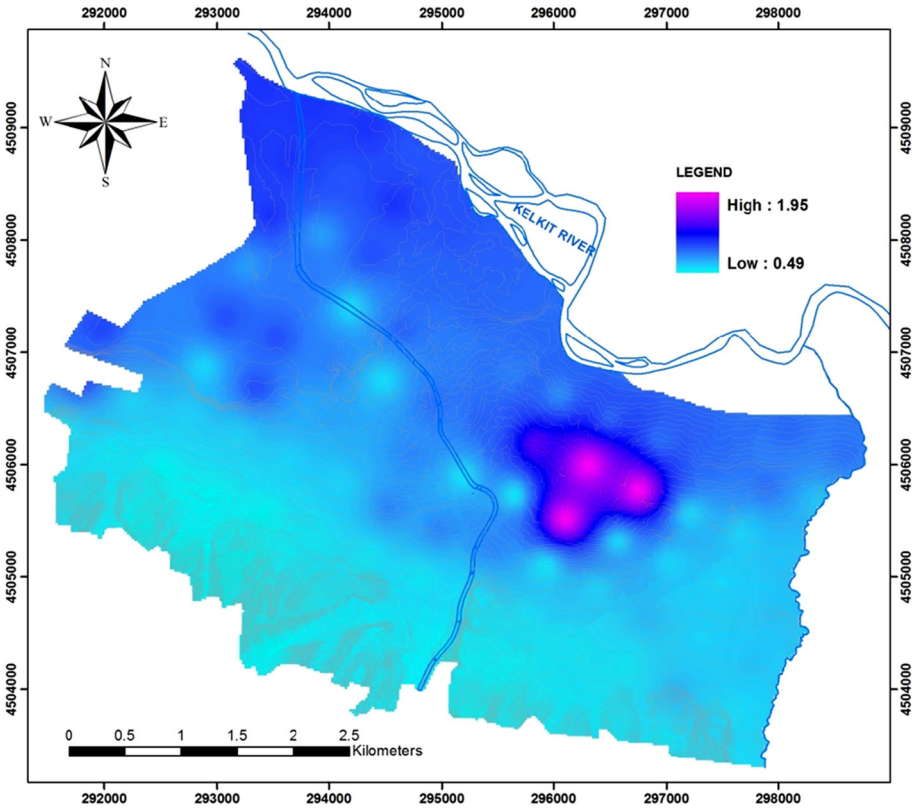

Fig. 25 Predominant period map of the study area (for CB08 model)

Table 9 Correlations of relative amplification factors with average shear wave velocity (after TCEGE, 1999)

Researcher(s)	Equation	
Midorikawa (1987)	$A = 68\ V_1^{-0.6}$	($V_1 < 1100$ m/s)
	$A = 1$	($V_1 > 1100$ m/s)
Joyner and Fumal (1984)	$A = 23\ V_2^{-0.45}$	
Borcherdt et al. (1991)	$\text{AHSA} = 700/V_1$	(for weak motion)
	$\text{AHSA} = 600/V_1$	(for strong motion)

A, Relative amplification factor for peak ground velocity; AHSA, average horizontal spectral amplification in period range of 0.4–2.0 s; V_1, average shear wave velocity over a depth of 30 m (in m/s), V_2, average shear wave velocity over a depth of one-quarter wavelength for a one-second period wave (in m/s)

7 Conclusions

Dynamic properties of the Erbaa soils were determined and shear wave velocity profiles prepared for one-dimensional site response analyses. During this process, empirical shear wave velocities were calculated and site-specific formulas proposed. 1-D equivalent linear

Table 10 The amplification results for each borehole for the study area

BH-no	Amplification factor	BH-no	Amplification factor	BH-no	Amplification factor	BH-no	Amplification factor
1	2.59	27	2.46	53	2.11	79	2.09
2	2.30	28	2.57	54	2.44	80	2.36
3	2.38	29	2.41	55	2.33	81	2.26
4	2.88	30	2.41	56	2.27	82	2.29
5	2.48	31	2.34	57	2.27	83	2.26
6	2.83	32	2.42	58	2.17	84	2.23
7	2.53	33	2.26	59	2.21	85	2.02
8	2.81	34	2.40	60	2.32	86	1.94
9	2.45	35	2.32	61	2.26	87	2.27
10	2.43	36	2.53	62	2.38	88	2.33
11	2.40	37	2.56	63	2.19	89	2.38
12	2.05	38	2.44	64	2.12	90	2.40
13	2.31	39	2.40	65	2.27	91	2.21
14	2.21	40	2.43	66	2.17	92	2.06
15	2.31	41	2.33	67	2.09	93	2.27
16	2.34	42	2.39	68	2.09	94	2.23
17	2.35	43	2.28	69	2.19	95	2.50
18	2.59	44	2.52	70	2.26	96	2.47
19	2.45	45	2.42	71	1.92	97	2.53
20	2.42	46	2.33	72	2.06	98	2.56
21	2.41	47	2.28	73	2.23	99	2.53
22	2.38	48	2.43	74	2.26	100	2.51
23	2.28	49	2.32	75	1.97	101	2.53
24	2.39	50	2.16	76	2.03	102	2.53
25	2.36	51	2.20	77	2.23	103	2.47
26	2.20	52	2.38	78	2.15	104	2.52

site response analyses were performed in accordance with site-specific grid models using ProSHAKE (v.1.12) software. In the site response analyses of Erbaa, input ground motions were characterized by PGA values.

Amplification factors are defined by different empirical approaches. Amplification factors from 1-D site response analyses and from different empirical approaches were found to vary within a range of approximately 0.5–2.5 in the study area. High amplification factors at some locations is due to the presence of higher thickness of loose alluvial materials and lower SPT N values, which results in low shear wave velocities. High amplification values can be expected in the alluvial units in the study area in accordance with two different NGA-based models (BA08 model and CB08 model). It is more preferable to use the results of site response analyses obtained from 1-D analyses.

The amplitude and frequency content of ground motions are both important for design of structures. The amplification ratio and predominant site period distributions suggest that high ratios and lower predominant site periods are dominant in the southern part of the study area.

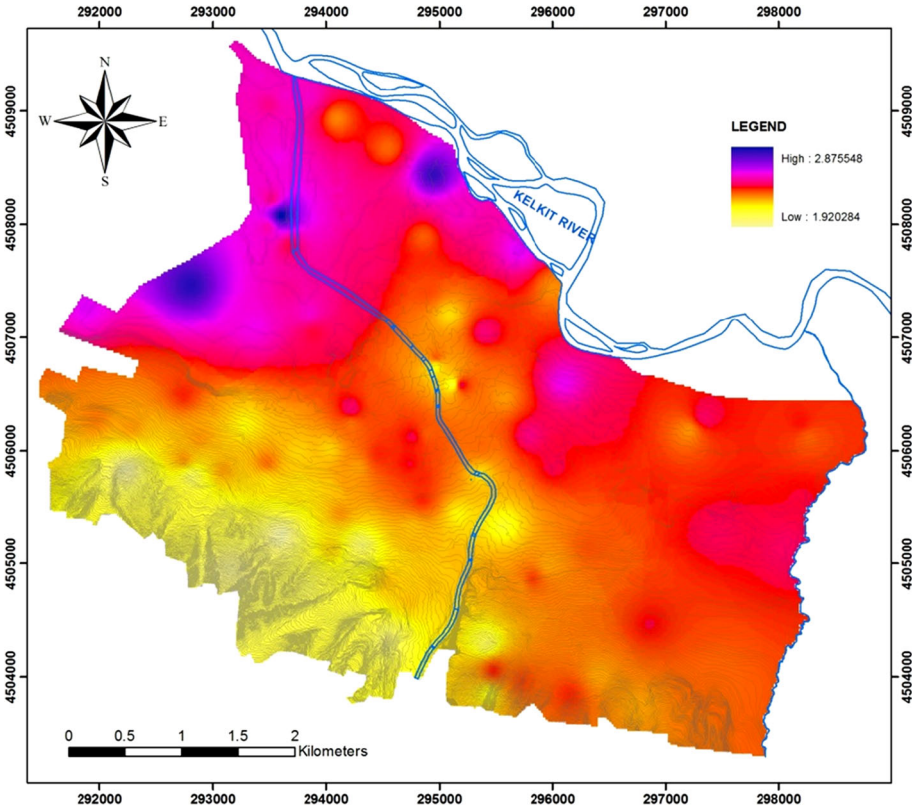

Fig. 26 Amplification factor map of the study area based on Midorikawa (1987) shear wave velocity relationship

Table 11 Comparison of amplification and predominant periods based on different methods

Methods	Amplification			Predominant periods		
	Min	Max	Mean	Min	Max	Mean
1-D equivalent linear based (ProSHAKE v.1.12)						
BA08 Model	1.1	1.8	1.5	0.5	2.18	1.1
CB08 Model	1.1	1.8	1.6	0.5	1.95	1.1
V_s-Based empirical approach (Midorikawa 1987)	1.92	2.88	2.34	–	–	–

Acknowledgments This work has been supported by the Scientific and Technical Research Council of Turkey (TUBITAK) (TUBITAK-CAYDAG No: 107Y068), the Research Foundation of Middle East Technical University (BAP No: 2009-03-09-01) and the Research Foundation of the Prime Ministry State Planning Organization (DPT No: CUBAP M-359/DPT 2006 K-120220). The authors gratefully acknowledge Prof. Dr. Orhan Tatar from Cumhuriyet University for his support during the DPT project. The Fulbright program gave the opportunity to make this research mutually and internationally possible in USA. The authors would like to thank the anonymous reviewers for their comments.

References

Akın M (2009) Seismic Microzonation of Erbaa (Tokat-Turkey) Located Along Eastern Segment of the North Anatolian Fault Zone, PhD Dissertation, Middle East Technical University

Akin M, Kramer SL, Topal T (2009) Comparison of measured and estimated shear wave velocities in a seismically active area (Erbaa, Turkey). Fifth international conference on recent advances in geotechnical earthquake engineering and soil dynamics, San Diego, California

Akin KM, Kramer SL, Topal T (2011a) Empirical correlations of shear wave velocity (V_s) and penetration resistance (SPT-N) for different soils in an earthquake-prone area (Erbaa-Turkey). Eng Geol 119(1–2):1–17

Akin KM, Topal T, Kramer SL (2011b) Seismic microzonation of Erbaa, Tokat, Turkey based on analytical hierarchical process (AHP). Environ Eng Geosci 18:191–207

Akin KM, Topal T, Kramer SL (2013) A newly developed seismic microzonation model of Erbaa (Tokat, Turkey) located on seismically active eastern segment of the North Anatolian Fault Zone (NAFZ). Nat Hazards 65(3):1411–1442

Aktimur T, Ates S, Yurdakul E, Tekirli E, Kecer M (1992) Niksar-Erbaa ve Destek Dolayinin Jeolojisi. MTADergisi, 114 (in Turkish)

Allen CR (1969) Active faulting in Northern Turkey, Division of Geological Science, California Institute of Technology, Contr. No. 1577

Ambraseys NN (1970) Some characteristic features of the North Anatolian fault zone. Tectonophysics 9:143–165

Ansal A, Tonuk G (2007) Source and site factors in microzonation. In: Pitilakis KD (ed) Earthquake geotechnical engineering, 4th international conference on earthquake geotechnical engineering-invited lectures, pp 73–92

Ansal A, Tonuk G, Demircioglu M, Bayraklı Y, Sesetyan K, Erdik M (2006) Ground motion parameters for vulnerability assessment. Proceedings of the First European Conference on Earthquake Engineering and Seismology, Geneva, Switzerland, Paper Number: 1790

ASTM D 5778-95 (2000) Standard test method for performing electronic friction cone and piezocone penetration testing of soils. ASTM, West Conshohocken, PA

Athanasopoulos GA (1995) Empirical correlations Vs-NSPT for soils of Greece: a comparative study of reliability. In: Cakmak AS (ed) Proceedings of 7th ınternational conference on soil dynamics and earthquake engineering (Chania, Crete). Computational Mechanics, Southampton, pp 19–36

Bang E, Kim D (2007) Evaluation of shear wave velocity profile using SPT-based uphole method. Soil Dyn Earthq Eng 27:741–758

Barka AA, Akyüz SH, Cohen HA, Watchorn F (2000) Tectonic evolution of the Niksar and Taşova-Erbaa pull-apart basins, North Anatolian Fault Zone: their significance for the motion of the Anatolian block. Tectonophysics 322:243–264

Boore DM, Atkinson GM (2008) Ground-motion prediction equations for the average horizontal component of PGA, PGV, and 5%-damped PSA at spectral periods between 0.01 and 10.0 s. Earthquake Spectra 24(1):99–138

Borcherdt RD (1970) Effects of local geology on ground motion near San Francisco Bay. Bull Seismol Soc Am 60:29–61

Borcherdt RD (1994) Estimates of site depending response spectra for design methodology and justifications. Earthquake Spectra 10(4):617–654

Borcherdt RD, Wentworth CM, Janssen A, Fumal T, Gibbs J (1991) Methodology for predictive GIS mapping of special study zones for strong ground shaking in the San Francisco bay region. In: Proceedings of fourth ıntern'l. conference on seisimc zonation vol 3, pp 545–552

Cabalar AF, Cevik A (2009) Genetic programming-based attenuation relationship: an application of recent earthquakes in Turkey. Comput Geosci 9:1884–1896

Campbell KW, Bozorgnia Y (2008) NGA ground motion model for the geometric mean horizontal component of PGA, PGV, PGD, and 5% damped linear elastic response spectra for periods ranging from 0.01 to 10 s. Earthquake Spectra 24(1):139–171

Castro RR, Anderson JG, Singh SK (1990) Site response, attenuation and source spectra of S-waves along the Guerrero, Mexico subduction zone. Bull Seismol Soc Am 79:1481–1503

Darendeli MB (2001) Development of a new family of normalized modulus reduction and material damping curves. PhD Dissertation, The University of Texas at Austin

Dikmen U (2009) Statistical correlations of shear wave velocity and penetration resistance for soils. J Geophys Eng 6:61–72

Dobry R, Borcherdt RD, Crouse CB, Idriss IM, Joyner WB, Martin GR, Power MS, Rinne EE, Seed RB (2000) New site coefficient and site classification system used in recent building code provisions. Earthq Spectra 16(1):41–67

EPRI (1993) Guidelines for determining design basis ground motions. Vol. 1: method and guidelines for estimating earthquake ground motion in eastern North America, Rpt. No. EPRI TR-102293, Palo Alto, California

Erdik M, Doyuran V, Gülkan P, Akkas N (1985) A probabilistic assessment of the seismic hazard in Turkey. Tectonophysics 117:295–344

Erdik M, Demircioglu M, Sesetyan K, Durukal E (2005) Assessment of earthquake hazard for Bakirkoy, Gemlik, Bandırma, Tekirdag and Korfez. WB MEER project-A3 component, microzonation and Hazard Vulnerability Studies for Disaster Mitigation in Pilot Municipalities, Bogazici University, Kandilli Observatory and Earthquake Engineering Research Institute

Ergin M, Ozalaybey S, Aktar M, Yakin MN (2004) Site amplification at Avcilar, Istanbul. Tectonophysics 391:335–346

Fujiwara T (1972) Estimation of ground movements in actual destructive earthquakes. Proceedings of the fourth European symposium on earthquake engineering, London, pp 125–132

Fumal TE, Tinsley JC (1985) Mapping shear wave velocities of near surface geological materials. In: Ziony TI (ed) Predicting areal limits of earthquake induced landsliding. In evaluation of earthquake hazards in the Los Angeles region—an earth science perspective, USGS Paper 1360, pp 127–150

General Directorate of Disaster Affairs (2008) www.deprem.gov.tr/indexen.html, 01.02. 2008

Hanumantharao C, Ramana GV (2008) Dynamic soil properties for microzonation of Delhi, India. J Earth Syst Sci 117(S2):719–730

Hasançebi N, Ulusay R (2007) Empirical correlations between shear wave velocity and penetration resistance for ground shaking assessments. Bull Eng Geol Environ 66:203–213

Humphrey JR, Anderson JG (1992) Shear wave attenuation and site response in Guerrero, Mexico. Bull Seismol Soc Am 82:1622–1645

Imai T (1977) P and S wave velocities of the ground in Japan. Proceeding of IX international conference on soil mechanics and foundation engineering, vol 2, pp 127–132

Imai T, Tonouchi K (1982) Correlation of N-value with S-wave velocity and shear modulus. Proceedings of the 2nd European symposium of penetration testing, Amsterdam, pp 57–72

Imai T, Yoshimura Y (1970) Elastic wave velocity and soil properties in soft soil. Tsuchito-Kiso 18(1):17–22 **(in Japanese)**

Imai T, Fumoto H, Yokota K (1975) The relation of mechanical properties of soil to P- and S- wave velocities in Japan. In: Proceedings of 4th Japan earthquake engineering symposium, pp 89–96 (in Japanese)

Iyisan R (1996) Correlations between shear wave velocity and in situ penetration test results. Chamber of Civil Engineers of Turkey. Teknik Dergi 7(2), 1187-1199 (in Turkish)

Jafari MK, Asghari A, Rahmani I (1997) Empirical correlation between shear wave velocity (Vs) and SPT-N value for south of Tehran soils. In: Proceedings of 4th ınternational conference on civil engineering (Tehran, Iran) (in Persian)

Jafari MK, Shafiee A, Razmkhah A (2002) Dynamic properties of fine grained soils in south of Tehran. J Seismol Earthq Eng 4:25–35

Jinan Z (1987) Correlation between seismic wave velocity and the number of blow of SPT and depth. Selected Papers from the Chinese Journal of Geotechnical Engineering, pp 92–100

Joyner WB, Fumal TE (1984) Use of measured shear-wave velocity for predicting geologic site effects on strong ground motion. In: Proceedings of eighth world conference on earthquake engineering, Vol. II, 777–783

Kalteziotis N, Sabatakakis N, Vassiliou J (1992) Evaluation of dynamic characteristics of greek soil formations. In: Second hellenic conference on geotechnical engineering vol 2, pp. 239–246 (in Greek)

Kanai K (1966) Conference on cone penetrometer the ministry of public works and settlement (Ankara, Turkey) (presented by Y Sakai, 1968)

Kayabalı K (1996) Soil liquefaction evaluation using shear wave velocity. Eng Geol 44(1):121–127

Ketin I (1969) Kuzey Anadolu Fayı Hakkında. MTA Dergisi 72:1–25 **(in Turkish)**

Kiku H, Yoshida N, Yasuda S, Irisawa T, Nakazawa H, Shimizu Y, Ansal A, Erkan A (2001) In-situ penetration tests and soil profiling in Adapazari, Turkey. In: Proceedings of the ICSMGE/TC4 satellite conference on lessons learned from recent strong earthquakes, pp 259–265

Kim DS, Bang ES, Seo WS (2004) Evaluation of shear wave velocity profile using SPT-Uphole method. International site characterization, ISC-2 Porto, Portugal, pp 339–344

Kramer SL (1996) Geotechnical earthquake engineering. Prentice Hall, USA

Kramer SL, Stewart JP (2004) Geotechnical aspects of seismic hazards. In: Bozorgnia Y, Bertero VV (eds) Earthquake engineering from engineering seismology to performance-based engineering, CRC Press, Chapter 4

Lee SH (1990) Regression models of shear wave velocities. J. Chin. Inst. Eng. 13:519–532

Matsuoka M, Wakamatsu K, Fujimoto K, Midorikawa S (2006) Average shear-wave velocity mapping using Japan engineering geomorphologic classification map. J Struct Mech Earthq Eng JSCE 23(1):57–68

Midorikawa S (1987) Prediction of isoseismal map in the Kanto plain due to hypothetical earthquake. J Struct Eng 33B:43–48

Moehle J (1994) Preliminary report on the seismological and engineering aspects of January 17, 1994 Northridge Erathquake. University of Calif, at Berkeley, Earthquake Engineering Research Center, Report No. UCB/EERC-94/01

Ohba S, Toriumi I (1970) Dynamic response characteristics of Osaka Plain. Proceedings of the annual meeting, A. I. J. (in Japanese)

Ohsaki Y, Iwasaki R (1973) On dynamic shear moduli and Poisson's ratio of soil deposits. Soil Found 13:61–73

Ohta Y, Goto N (1978) Empirical shear wave velocity equations in terms of characteristics soil indexes. Earthq Eng Struct Dyn 6:167–187

Ohta T, Hara A, Niwa M, Sakano T (1972) Elastic shear moduli as estimated from N-value. In: Proceedings of 7th annal convention of Japan society of soil mechanics and foundation engineering, pp 265–268

Ohta Y, Goto N, Kagami H, Shiono K (1978) Shear wave velocity measurement during a standard penetration test. Earthq Eng Struct Dyn 6:43–50

Okamoto T, Kokusho T, Yoshida Y, Kusuonoki K (1989) Comparison of surface versus subsurface wave source for P–S logging in sand layer. In: Proceedings of 44th annal conference JSCE, vol 3, pp 996–997 (in Japanese)

Ozel O, Sasatani T (2004) A site effect study of the Adapazari basin, Turkey, from strong and weak-motion data. J Seismol 8(4):559–572

Pavlenko OV (2008) Characteristics of soil response in near-fault zones during the 1999 Chi–Chi, Taiwan earthquake. Pure Appl Geophys 165(9–10):1789–1812

Pitilakis K (2004) Site effects. In: Ansal A (ed) Recent advances in earthquake geotechnical engineering and microzonation. Springer, Netherlands, pp 139–197

Pitilakis KD, Anastasiadis A, Raptakis D (1992) Field and laboratory determination of dynamic properties of natural soil deposits. In: Proceedings of 10th world conference earthquake engineering, Rotherdam, pp 1275–1280

Pitilakis K, Raptakis D, Lontzetidis KT, Vassilikou T, Jongmans D (1999) Geotechnical and geophysical description of Euro-Seistests, using field and laboratory tests, and moderate strong ground motions. J Earthq Eng 3:381–409

Raptakis DG, Anastasiadis SAJ, Pitilakis KD, Lontzetidis KS (1995) Shear wave velocities and damping of Greek natural soils. In: Proceedings of 10th European conference of earthquake engineering, Vienna, pp 477–482

Seed HB, Idriss IM (1981) Evaluation of liquefaction potential sand deposits based on observation of performance in previous earthquakes. ASCE National Convention (MO), pp 481–544

Seed HB, Sun JH (1989) Implication of site effects in the Mexico City earthquake of September 19, 1985 for Earthquake-Resistant Design Criteria in the San Francisco Bay Area of California, Report No. UCB/EERC-89/03, Earthquake Engineering Research Center, University of California, Berkeley

Seed RB, Dickenson SE, Riemer MF, Bray JD, Sitar N, Mitchell JK, Idriss IM, Kayen RE, Kropp AK, Harder LF, Power MS (1990) Preliminary report on the principle geotechnical aspects of the October 17, 1989 Loma Prieta earthquake, Report No. UCB/EERC-90/05, Earthquake Engineering Research Center, University of California, Berkeley

Seed HB, Idriss IM, Arango I (1983) Evaluation of liquefaction potential using field performance data. J Geotech Eng ASCE 109:458–482

Şengör AMC, Görür N, Şaroğlu F (1985) Strike-slip faulting and related basin formation in zones of tectonic escape: Turkey as a case study, Strike-slip deformation, basin formation, and sedimentation, Soc. Econ. Paleont. Min. Spec. Pub. 37 (in honor of J.C. Crowell), pp 227–264

Şengör AMC, Tüysüz O, İmren C, Sakınç M, Eyidoğan H, Görür N, Le Pichon X, Rangin C (2005) The North Anatolian fault: a new look. Annu Rev Earth Planet Sci 33:37–112

Shibata T (1970) Analysis of liquefaction of saturated sand during cyclic loading. Disaster Prevention Res Inst Bull 13:563–570

Sisman H (1995) An investigation on relationships between shear wave velocity, and SPT and pressuremeter test results. MSc Thesis, Ankara University, Geophysical Engineering Department, Ankara, 75 pp (in Turkish)

Stein RS, Barka AA, Dieterich JH (1997) Progressive failure on the North Anatolian fault since 1939 by earthquake stress triggering. Geophys J Int 128:594–604
Sykora DE, Stokoe KH (1983) Correlations of in situ measurements in sands of shear wave velocity. Soil Dyn Earthq Eng 20:125–136
Takemiya H, Adam M (1997) Seismic wave amplification due to topography and geology in Kobe during Hyogo-Ken Nanbu Earthquake. J Struct Mech Earthq Eng 14(2):129–138
Tatar O, Piper JDA, Park RG, Gürsoy H (1995) Paleomagnetic study of block rotations in the Niksar overlap region of the North Anatolian Fault Zone, central Turkey. Tectonpysics 244:251–266
TCEGE (1999) Manual for zonation on seismic geotechnical hazards. Publication of the Japanese Geotechnical Society, Revised Version
Tezcan SS, Kaya E, Bal İE, Özdemir Z (2002) Seismic amplification at Avcılar, Istanbul. Eng Struct 22:661–667
Tonouchi K, Sakayama T, Imai T (1983) S wave velocity in the ground and the damping factor. Bull Int Assoc Eng Geol 26–27:327–333
U.S. Army Corps of Engineers (1999) Engineer manual, EM1110-2-6050, engineering and design: response spectra and seismic analysis for concrete hydraulic structures, 30 June 1999, Washington, DC 20314-1000
Vucetic M, Dobry R (1991) Effect of soil plasticity on cyclic response. J Geotech Eng ASCE 117:87–107
Westaway R (2003) Kinematics of the middle east and eastern mediterranean updated. Turkish J Earth Sci 12:5–46
EduPro Civil Systems, Inc. ProShake version 1.12, Ground Response Analyses Program, Sammamish, Washington, USA
Yılmaz I (1998) Köklüce regülatörü-Erbaa HES iletim hattı güzergahındaki alüvyal zeminlerin şişme ve oturma sorunlarının jeomühendislik değerlendirmesi: Unpubl. Ph.D. thesis, Cumhuriyet University, Sivas (in Turkish)
Yokota K, Imai T, Konno M (1991) Dynamic deformation characteristics of soilsdetermined by laboratory tests. OYO Tee Rep 3:13